Long-Term Memory in *Drosophila* Is Influenced by Histone Deacetylase HDAC4 Interacting with SUMO-Conjugating Enzyme Ubc9

Silvia Schwartz,* Mauro Truglio,* Maxwell J. Scott,† and Helen L. Fitzsimons*,[1]
*Institute of Fundamental Sciences, Massey University, Palmerston North 4442, New Zealand, and †Department of Entomology, North Carolina State University, Raleigh, North Carolina 27695-7613

ABSTRACT HDAC4 is a potent memory repressor with overexpression of wild type or a nuclear-restricted mutant resulting in memory deficits. Interestingly, reduction of HDAC4 also impairs memory via an as yet unknown mechanism. Although histone deacetylase family members are important mediators of epigenetic mechanisms in neurons, HDAC4 is predominantly cytoplasmic in the brain and there is increasing evidence for interactions with nonhistone proteins, suggesting HDAC4 has roles beyond transcriptional regulation. To that end, we performed a genetic interaction screen in *Drosophila* and identified 26 genes that interacted with *HDAC4*, including Ubc9, the sole SUMO E2-conjugating enzyme. RNA interference-induced reduction of *Ubc9* in the adult brain impaired long-term memory in the courtship suppression assay, a *Drosophila* model of associative memory. We also demonstrate that *HDAC4* and *Ubc9* interact genetically during memory formation, opening new avenues for investigating the mechanisms through which *HDAC4* regulates memory formation and other neurological processes.

KEYWORDS histone deacetylase; SUMOylation; plasticity; neuron; memory

THE histone deacetylase HDAC4 is widely expressed in neurons throughout the brain (Darcy *et al.* 2010) and an increasing body of evidence indicates that HDAC4 plays important roles in neurological function (Kumar *et al.* 2005; Chen and Cepko 2009; Kim *et al.* 2012; Li *et al.* 2012; Sando *et al.* 2012; Sarkar *et al.* 2014). To that end, we recently demonstrated that in *Drosophila*, RNA interference (RNAi)-mediated knockdown of *HDAC4* in the adult brain impairs long-term memory (LTM) in the courtship suppression assay, a model of associative memory (Fitzsimons *et al.* 2013). Similarly in humans, loss of one copy of *HDAC4* correlates with brachydactyly mental retardation syndrome (BDMR), the neurological symptoms of which include intellectual disability and autism (Williams *et al.* 2010; Morris *et al.* 2012; Villavicencio-Lorini *et al.* 2013), and in mice, conditional knockout of *HDAC4* in the brain results in impairments in hippocampal-dependent associative LTM (Kim *et al.* 2012). Despite this growing evidence of a critical role, the mechanism(s) through which HDAC4 positively influences LTM is unknown. This is in part because HDAC4 exists in both nuclear and cytoplasmic pools, and under basal conditions, the majority of HDAC4 is localized to the cytoplasm (Chawla *et al.* 2003; Darcy *et al.* 2010). Given the predominant nonnuclear localization, particularly the concentration of HDAC4 at dendritic spines (Darcy *et al.* 2010), we hypothesize that cytoplasmic HDAC4 is required in memory formation; however, the mechanisms through which HDAC4 acts outside the nucleus are unknown.

The nuclear role of HDAC4 is less of an enigma. When in the nucleus, HDAC4 acts as a transcriptional repressor; although vertebrate HDAC4 is catalytically inactive as a histone deacetylase, rather it facilitates changes in gene expression through direct binding and inhibition of transcription factors such as MEF2 (Miska *et al.* 1999; Wang *et al.* 1999; Lu *et al.* 2000). As described above, HDAC4 must be present for normal LTM; however, increased nuclear HDAC4 also impairs memory (Williams *et al.* 2010; Sando *et al.* 2012). An individual with BDMR was identified to carry a point mutation that resulted in a truncated HDAC4 protein (Williams *et al.* 2010), and

doi: 10.1534/genetics.115.183194
Manuscript received September 28, 2016; accepted for publication April 29, 2016; published Early Online May 3, 2016.
Supplemental material is available online at www.genetics.org/lookup/suppl/doi:10.1534/genetics.115.183194/-/DC1.
[1]Corresponding author: Institute of Fundamental Sciences, Massey University, Private Bag 11-222, Palmerston North 4442, New Zealand. E-mail: h.l.fitzsimons@massey.ac.nz

further investigation of a similar HDAC4 variant in the mouse revealed a gain of function, with this truncated protein lacking a nuclear export signal and thus being sequestered in the nucleus. The truncated form of HDAC4 also caused cognitive deficits in mice, which were associated with reduced expression of plasticity-related genes (Sando *et al.* 2012). We also demonstrated that overexpression of *HDAC4* in *Drosophila* resulted in impaired LTM and recruited MEF2 to discrete foci within nuclei (Fitzsimons *et al.* 2013). Taken together, these data indicate that when in the nucleus, HDAC4 has the capacity to repress expression of plasticity-related genes, which correlates with memory impairment (Sando *et al.* 2012); however, it also plays a promemory role, as evidenced by the memory impairments that result from reduction of HDAC4 in the adult brain (Kim *et al.* 2012; Fitzsimons *et al.* 2013).

Here, we sought to increase understanding of the molecular mechanisms through which HDAC4 regulates memory via a two-pronged approach. First, in order to investigate whether the memory deficits we observed following overexpression of *HDAC4* were accompanied by alterations in gene expression, we performed RNA sequencing (RNAseq) on heads of flies that overexpressed *HDAC4* in the adult brain; however, very few changes were found, suggesting that wild-type (WT) HDAC4 elicits limited transcriptional effects.

For our second approach, we sought to identify genes that interact with *HDAC4* by making use of a rough eye enhancer/suppressor screen, which would capture both transcriptional and nontranscriptional interactions. Our results indicate that HDAC4 interacts with genes that are important for transcription, the cytoskeleton, and SUMOylation. This study thus provides several new avenues for investigation of the mechanisms through which *HDAC4* regulates memory formation.

Materials and Methods

Fly strains

All flies were cultured on standard medium on a 12-hr light/dark cycle and maintained at a temperature of 25° unless otherwise indicated. The *UAS-HDAC4OE* transgenic line harbors a *UAS* upstream of WT *Drosophila HDAC4* fused to an N-terminal FLAG-tag, as previously described (Fitzsimons *et al.* 2013). *GMR-HDAC4* was generated by fusing *HDAC4* directly under control of *GMR* by standard methods; human *HDAC4* and *3SA* were cloned into pUASTattB by standard methods. The *UAS-HDAC4* and *GMR-HDAC4* transgenic flies were generated by GenetiVision (Houston, TX), using the P2 injection strain (attP insertion site 3L68A4). *elav^{c155}-GAL4* (no. 458), *GMR-GAL4* (no. 1104), *ey-GAL4* (no. 5535), *OK107-GAL4* (no. 854), and *tub-GAL80ts* (no. 7108) were obtained from the Bloomington *Drosophila* Stock Center (Bloomington, IN). All were outcrossed into the *w(CS10)* background. The *HDAC4*::*YFP* protein trap strain CPTI-000077 (no. 115008) was obtained from the Kyoto Stock Center. The *elav-GAL4*; *tub-GAL80ts* and *OK107-GAL4*; *tub-GAL80ts* lines were generated via standard genetic crosses, as were G*MR-GAL4*; *UAS-HDAC4OE* and *ey-GAL4*; *GMR-HDAC4*. Transgenic RNAi lines containing an inducible UAS-RNAi construct targeted to a single protein-coding gene were obtained from the Vienna *Drosophila* Resource Center (VDRC). Control crosses were performed with reference strain in the appropriate genetic background [*w(CS10)* or *w^{1118}*].

Transcriptome analysis

To express *HDAC4* in the adult brain, *UAS-HDAC4OE* flies (Fitzsimons *et al.* 2013) were crossed to *elav-GAL4*; *tub-GAL80ts* flies and raised at the permissive temperature of 19°. *w(CS10)* flies crossed to *elav-GAL4*; *tub-GAL80ts* served as the control. Three days after eclosion, flies were transferred to 30° to induce *HDAC4* expression. After 48 hr, three biological replicates (*i.e.*, from three separate crosses) were snap frozen in a dry ice/ethanol bath and vortexed to remove the heads. Heads were collected over dry ice and RNA was extracted with TRIzol and purified with an RNeasy microarray tissue mini kit (Qiagen, Valencia, CA). Whole heads were used in order to reduce variation from individual dissection of brains and this method has been successfully employed to analyze brain-specific changes in gene expression in *Drosophila* (Winbush *et al.* 2012). The high quality of the RNA was confirmed on a Bioanalyzer (Agilent). Illumina libraries were prepared with an Illumina RNA TruSeq kit and run on an Illumina HiSeq with three samples per lane (North Carolina State University Genomic Sciences Laboratory). Over 60 million 100-bp reads were obtained per sample, which were mapped to the *Drosophila* reference genome (release 5.41, FB2011_09; 15,438 predicted genes). The reads were mapped using TopHat and analyzed for reads alignment percentage and gene coverage (Trapnell *et al.* 2012). Data analysis was restricted to genes with fragment per kilobase of exon per million fragments mapped (FPKM) value of at least 1.0 as employed by the ModENCODE Consortium and in other studies (Roy *et al.* 2010; Winbush *et al.* 2012). The Cufflinks pipeline, version 2.2.1 was used to assemble mapped reads into transcripts, estimate their abundances, and test for differential expression between samples (Trapnell *et al.* 2012). Assemblies resulting from Cufflinks analysis were merged together using the Cuffmerge utility, which is included in the Cufflinks package. The merged assemblies were provided to Cuffdiff, a program included in the Cufflinks package that tests the statistical significance of each observed change in expression between the samples. The statistical model used to evaluate changes assumes that the number of reads produced by each transcript is proportional to its abundance. The expression level of transcripts across the runs was normalized by the total number of mapping reads using the FPKM normalization method (Mortazavi *et al.* 2008; Trapnell *et al.* 2012). Cuffdiff implements a linear statistical model to estimate an assignment of abundance to each transcript. Fold changes, expressed in $\log_2$ scale, raw *P*-values, and adjusted *Q*-values were calculated by standard methods. Plots were generated using the CummeRbund tool, which analyzes the Cuffdiff data into the R statistical

computing environment, helping visualize the data (R version 3.2.0). We observed that one of the three control samples displayed different FKPM distribution; therefore, we performed the analysis both including and excluding the control and we detected significant changes in transcript abundance in 32 genes, and 28 of these genes were still significantly differentially expressed when analyzed with all three controls.

Rough eye phenotype screen

All crosses were performed at 25°, unless otherwise stated. *GMR-GAL4*; *HDAC4OE* flies were crossed to each RNAi line and the eye phenotypes of progeny were assessed at ~7 days of age. Eyes were examined under a stereomicroscope (Olympus SZX12, DP controller imaging software, manual exposure, ISO 200, zoom 108 mm, exposure time 1/20 sec). A semi-quantitative scoring system was used to evaluate the rough eye phenotype by scoring bristles, ommatidia, pigmentation, and shape. *GMR-GAL4* flies were also crossed to each RNAi line to assess the effect of knockdown of each target gene on the eye phenotype (in the absence of *HDAC4* overexpression) and lines with more than a very mild rough eye were excluded. Similarly, *ey-GAL4*, *GMR-HDAC4* flies were crossed to appropriate RNAi lines and the eye phenotype was compared to that of *ey-GAL4*-driven expression of each RNAi line.

Quantitative RT-qPCR

The efficiency *of Ubc9* knockdown was examined by RT-qPCR. *elav-GAL4/+*; *tub-GAL80ts/Ubc9kd* flies and control *elav-GAL4/+*; *tub-GAL80ts/+* flies were raised at the permissive temperature of 19° and then adults were shifted to the restrictive temperature of 30° for 48 hr. Flies were snap frozen and heads collected over dry ice, and then total RNA was extracted from ~50 heads with TRIzol and quantified on a NanoDrop. Complementary DNA (cDNA) was synthesized with random primers (Sigma-Aldrich, St. Louis, MO) and Transcriptor Reverse Transcriptase (Sigma-Aldrich). For PCR amplification, the following primers were used: *Ubc9* 5′-ATTTCCGCTAGCA GTCCCAC-3′ and 5′-TGCTTGGAACCACTGGAGAC-3′; and *EF1a48D*, 5′-ACTTTGTTCGAATCCGTCGC-3′ and 5′-TACGC TTGTCGATACCACCG-3′. PCR was performed with SsoFast EvaGreen supermix (BioRad) on a Roche Lightcycler 480 Instrument II (Roche) under standard cycling conditions. Both primer sets were confirmed to yield one major band of the correct size via agarose gel electrophoresis and melt curve analysis. Standard curves for each primer set were generated using fivefold dilutions of cDNA, and primer efficiency was between 95 and 105%. The comparative Ct method (also known as the $2^{-\Delta\Delta Ct}$ method) was used to normalize *Ubc9* transcript levels to those of the housekeeping gene *EF1a48D*. The $2^{-\Delta\Delta Ct}$ of *EF1a48D* was set to 1. Data were collected from three independent RNA samples for each genotype, and significance was assessed by Mann–Whitney *U*-test, with the significance level set at $P < 0.05$.

Courtship suppression assay

The courtship suppression assay was performed as previously described (Fitzsimons and Scott 2011; Fitzsimons *et al.* 2013). Briefly, male flies to be tested were collected and housed in single vials for 4–6 days. For each experiment, control genotypes were tested at the same time as those expressing the RNAi. In all experiments, the scorer was blind to the genotype of the flies. All naïve and trained groups contained (n = 15–25) males. All experiments were performed under ambient light. For experiments using the TARGET system (McGuire *et al.* 2004), the temperature was modulated by placing flies at the permissive temperature of 19° (GAL80ts active) or the restrictive temperature of 30° (GAL80ts inactive), as appropriate. Unless otherwise indicated, for induction of transgene expression, flies were transferred to 30° 3 days prior to training to allow maximum GAL4-mediated expression of the UAS construct. Flies were trained at 30° in an incubator under white light and remained at 30° until 30 min before testing, at which time they were transferred to 25° for equilibration to the testing conditions. A courtship index (CI) was calculated as the percentage of the 10-min period spent in courtship behavior. In order to compare memory across genotypes, a memory index (MI) was calculated by dividing the courtship index (CI) of each test fly by the mean CI of the sham flies of the same genotype (CI_{test}/mCI_{sham}) (Mehren and Griffith 2004; Ejima *et al.* 2005, 2007). A score of 0 indicated the highest memory performance possible, and a score ≥1.0 indicated no memory. For statistical analyses, data were arcsine transformed in order to approximate a normal distribution and significance was assessed by one-way ANOVA with *post hoc* Tukey's honest significant difference (HSD) test or a Student's *t*-test (two tailed, unpaired) with the significance level set at $P < 0.05$.

Immunohistochemistry

Immunohistochemistry on whole mount brains was performed as previously described (Fitzsimons *et al.* 2013). Brains were incubated overnight at room temperature with primary antibody (mouse anti-FasII, Developmental Studies Hybridoma Bank, 1:100), and then incubated overnight at 4° with secondary antibody (goat anti-mouse Alexa555, 1:500; Molecular Probes, Eugene, OR) and mounted with Antifade. For confocal microscopy, optical sections were taken with a Leica TCS SP5 DM6000B confocal microscope. Image stacks were taken at intervals of 1 μm and processed with Leica Application Suite Advanced Fluorescence (LAS AF) software.

Luciferase assay

Whole cell extracts were prepared from ~50 snap-frozen heads by homogenizing heads in 1× Reporter Lysis Buffer (Promega, Madison, WI) with a disposable mortar and pestle, and then centrifuging at 12,000 × *g* for 5 min at 4°. A total of 2 μl of lysate was incubated in a well of a 96-well plate with 50 μl Bright Glo (Promega). Luminescence was measured on a POLARstar Omega microplate reader (BMG Labtech). All samples were assayed in triplicate.

Western blotting

Whole cell extracts were prepared from 50–100 snap-frozen heads by homogenizing heads in 50 μl of RIPA buffer

Table 1 Genes with transcripts that differ significantly in abundance on overexpression of *HDAC4*

FlyBase ID	Gene name	Log_2 fold change	*P*-value	*Q*-value	Molecular function/biological process
FBgn0030773	*CG9676*	1.17	5.00E-5	0.0160689	Serine-type endopeptidase activity/proteolysis
FBgn0041210	*Histone deacetylase 4*	1.09	5.00E-5	0.0160689	Histone deacetylase activity/long-term memory; regulation of transcription, DNA templated
FBgn0041210	*CG11211*	1.07	5.00E-5	0.0160689	Carbohydrate binding; mannose binding/unknown
FBgn0040733	*CG15068*	1.03	5.00E-5	0.0160689	Unknown/unknown
FBgn0032507	*CG9377*	0.95	5.00E-5	0.0160689	Unknown/unknown
FBgn0026314	*UDP-glycosyltransferase 35b*	0.94	5.00E-5	0.0160689	UDP glycosyltransferase activity, transferring hexosyl groups/UDP glucose metabolic process
FBgn0040502	*CG8343*	0.89	5.00E-5	0.0160689	Carbohydrate binding; mannose binding/unknown
FBgn0036022	*CG8329*	0.84	5.00E-5	0.0160689	Serine-type endopeptidase activity/proteolysis
FBgn0039800	*Niemann-Pick type C-2g*	0.80	5.00E-5	0.0160689	Sterol binding/hemolymph coagulation; mesoderm development; sterol transport
FBgn0036015	*CG3088*	0.71	5.00E-5	0.0160689	Unknown/unknown
FBgn0013307	*Ornithine decarboxylase 1*	0.69	5.00E-5	0.0160689	Ornithine decarboxylase activity/polyamine biosynthetic process
FBgn0038516	*CG5840*	0.68	5.00E-5	0.0160689	Pyrroline-5-carboxylate reductase activity/oxidation reduction process; proline biosynthetic process
FBgn0003996	*white*[a]	0.67	5.00E-5	0.0160689	Eye pigment precursor/eye pigment precursor transporter activity
FBgn0040606	*CG6503*	0.67	5.00E-5	0.0160689	Unknown/unknown
FBgn0052667	*Short spindle 7*	0.66	5.00E-5	0.0160689	Unknown/mitotic spindle assembly; multicellular organism reproduction
FBgn0039684	*Odorant-binding protein 99d*	−1.68	5.00E-5	0.0160689	Odorant binding/autophagic cell death, intermale aggressive behavior
FBgn0002565	*Larval serum protein 2*	−1.38	5.00E-5	0.0160689	Nutrient reservoir activity/motor neuron axon guidance; synaptic target inhibition
FBgn0036659	*CG9701*	−1.35	5.00E-5	0.0160689	Hydrolase activity, hydrolyzing O-glycosyl compounds/ carbohydrate metabolic process
FBgn0027584	*CG4757*	−1.27	5.00E-5	0.0160689	Carboxylic ester hydrolase activity/unknown
FBgn0037683	*CG18473*	−1.27	5.00E-5	0.0160689	Aryldialkylphosphatase activity; hydrolase activity; zinc ion binding/catabolic process
FBgn0036106	*CG6409*	−0.90	5.00E-5	0.0160689	Unknown/GPI anchor biosynthetic process
FBgn0002526	*Laminin A*	−0.77	5.00E-5	0.0160689	Receptor binding/axon guidance; brain morphogenesis, cell adhesion by integrin; intermale aggressive behavior; locomotion involved in locomotory behavior; negative regulation of synaptic growth at neuromuscular junction
FBgn0015400	*Kekkon-2*	−0.72	5.00E-5	0.0160689	Unknown/unknown
FBgn0027843	*Carbonic anhydrase 2*	−0.71	5.00E-5	0.0160689	Carbonate dehydratase activity; one carbon metabolic process
FBgn0033926	*Activity-regulated cytoskeleton associated protein 1*	−0.69	5.00E-5	0.0160689	Nucleic acid binding/zinc ion binding; behavioral response to starvation; muscle system process
FBgn0034470	*Odorant-binding protein 56d*	−0.68	5.00E-5	0.0160689	Odorant binding/olfactory behavior; response to pheromone; sensory perception of chemical stimulus
FBgn0040211	*Homogentisate 1,2-dioxygenase*	−0.55	1.50E-4	0.0414082	Homogentisate 1,2-dioxygenase activity; L-phenylalanine catabolic process; oxidation-reduction process, tyrosine catabolic and metabolic process
FBgn0051205	*CG31205*	−0.54	1.50E-4	0.0414082	Serine-type endopeptidase activity/proteolysis

[a] *white* was used as an eye color selectable marker and is differentially expressed in the *HDAC4OE* and control samples, with *HDAC4OE* flies harboring three copies of w^+, in comparison to two in the control (genotypes: *w[CS10],elav/+*; *GAL80ts/+*; *HDAC4OE/+* and *w[CS10]elav/+*; *GAL80ts/+*).

± 10 mM N-ethylmaleimide (NEM) with a disposable mortar and pestle, and then centrifuging at 12,000 × *g* for 15 min at 4°. A total of 30 μg of each sample was loaded onto a 4–20% SDS-PAGE gel (BioRad) and resolved at 180 V. Protein was transferred onto nitrocellulose and blocked for >1 hr in 5% skim milk powder in TBST (50 mM Tris, 150 mM NaCl, 0.05% Tween-20, pH 7.6). The membrane was incubated overnight at 4° in primary antibody and 1 hr in secondary anti-mouse or anti-rabbit HRP-conjugated antibodies (GE Life Sciences) as appropriate. Antibodies used were rabbit anti-SUMO (kind gift from Albert Courey, University of California, Los Angeles; 1:5000) (Smith *et al.* 2004), rabbit anti-CaMKII (Cosmo Bio, 1:500), mouse anti-CREB (48H2 clone, Cell Signaling Technology, 1:1000), rabbit anti-MEF2 (kind

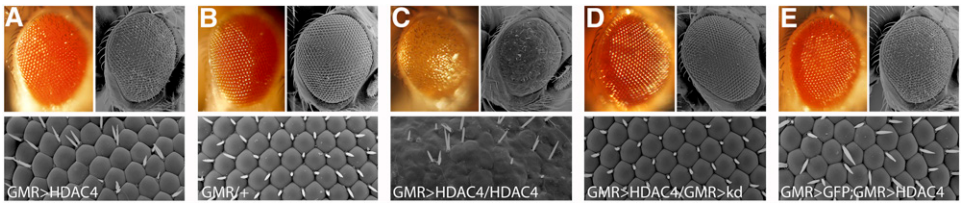

Figure 1 Rough eye phenotypes associated with overexpression of *HDAC4*. Stereomicrographs and scanning electron micrographs of *Drosophila* eyes. (A) *GMR-GAL4/+; UAS-HDAC4/+* flies display a mild rough eye phenotype. (B) This phenotype is not observed in control *GMR-GAL4* heterozygotes. (C) A second copy of *HDAC4* enhances the rough eye phenotype. (D) Coexpression of *UAS-HDAC4* and an RNAi hairpin targeted to *HDAC4* (kDa) restores with WT eye. (E) Coexpression of *UAS-HDAC4* with a second *UAS* construct (*GFP*) does not alter the rough eye phenotype.

gift from Bruce Paterson, 1:1000) (Lilly *et al.* 1995), and mouse anti-α-tubulin (12G10 clone, Developmental Studies Hybridoma Bank, 1:500) obtained from the Developmental Studies Hybridoma Bank developed under the auspices of the National Institute of Child Health and Human Development and maintained by the University of Iowa, Department of Biology, Iowa City, IA. Detection was performed with Amersham ECL Select or ECL Plus (GE Life Sciences).

Immunoprecipitation

The HDAC4::EYFP fly strain (Cambridge Protein Trap Project) was used for immunoprecipitation (IP) of HDAC4. This consists of an artificial exon containing the EYFP gene flanked by splice acceptor and donor sequences, which is inserted into the endogenous HDAC4 gene, resulting in an internal incorporation of EYFP into the HDAC4 protein (Knowles-Barley *et al.* 2010; Fitzsimons *et al.* 2013). Whole cell extracts from ∼100 heads were prepared as per the Western blotting method above. IP was performed with the Pierce Classic IP Kit (Thermo Scientific) according to the manufacturer's instructions. One microliter of anti-GFP antibody (Invitrogen, Carlsbad, CA) was incubated overnight with 600 μg of lysate. Following elution in 2× sample buffer, IP samples were processed for SDS-PAGE and Western blotting with anti-GFP (1:1000) or anti-SUMO (1:5000) antibodies alongside 30-μg input samples. Anti-α-tubulin (1:500) was used as a loading control.

Data availability

The authors state that all data necessary for confirming the conclusions presented in the article are represented fully within the article.

Results

Identification of HDAC4 gene targets in neurons

We initially sought to examine whether HDAC4 regulates transcription in the *Drosophila* brain and if so, to identify the specific gene targets. In order to compare transcript abundance between control and *HDAC4*-overexpressing flies, we expressed *HDAC4* with the panneuronal *elav* driver (Robinow and White 1991) and induced expression in the adult brain with the TARGET system (McGuire *et al.* 2004). Analysis of differential expression confirmed that *HDAC4* was significantly overexpressed by approximately twofold, but we did not observe global changes in gene expression. Thirteen genes (excluding *HDAC4* and *white*, which was the selectable marker for transgenesis) were increased in abundance and 13 were decreased (Table 1). Of the putative *HDAC4* transcriptional targets, few have been implicated in neurological functioning. The mammalian homolog of activity-regulated cytoskeleton-associated protein 1 (*Arc1*) is an immediate-early gene that is essential for synaptic plasticity and long-term memory and its expression is positively regulated by MEF2 in neurons (Flavell *et al.* 2006); therefore, it is likely that HDAC4 reduces *Arc1* expression by direct inhibition of MEF2. However *Arc1* mutants did not display impaired synaptic plasticity in *Drosophila* (Mattaliano *et al.* 2007).

A screen for modifiers of the HDAC4-induced rough eye phenotype

As genetic screens can identify genes that interact through nontranscriptional mechanisms (Kaplow *et al.* 2007; Cao *et al.* 2008; Kim *et al.* 2010), and given that we detected minimal changes in gene expression at the transcriptional level, we elected to perform a rough eye enhancer genetic screen on a panel of RNAi lines. We observed that overexpression of *HDAC4* in the eye with the glass multimer reporter driver (*GMR-GAL4*) (Freeman 1996) results in a rough eye phenotype, with disorganized ommatidia and bristles (Figure 1A) compared to the *GMR-GAL4* control (Figure 1B). How increased HDAC4 specifically disrupts eye development is unknown; however, known HDAC4 interactors including MEF2, CREB, Gcn5, and 14-3-3ζ have been identified to play roles in the development of photoreceptors, which are specialized neurons (Kockel *et al.* 1997; Anderson *et al.* 2005; Andzelm *et al.* 2015). The severity of the phenotype correlated with the dose of *HDAC4*, as flies harboring two copies of *UAS-HDAC4* displayed a severe phenotype, with fusion of most ommatidia, widespread bristle loss, and severely reduced pigmentation (Figure 1C). Thus the mild rough eye observed with one copy of *UAS-HDAC4* provides an ideal system for screening for modifiers as it allows for easy identification of enhancers of this phenotype. Further, as expression is predominantly restricted to the eye, the flies are viable and fertile. When an inverted repeat RNAi targeted to *HDAC4* was cointroduced with *UAS-HDAC4*, the eye phenotype was restored to WT (Figure 1D), confirming that the rough eye phenotype was a result of *HDAC4* expression and not caused by nonspecific effects. As the presence of a second *UAS* line could theoretically decrease *HDAC4* expression due to titration of GAL4, (rather

Table 2 Genes previously identified to interact with *hdac4* that also interact genetically with *HDAC4* in *Drosophila*

Gene name	Annotation symbol	VDRC/BDSC no.	Method	Molecular function
Gcn5 (PCAF)	CG4107	VDRC 21786	RNAi	H4 histone acetyltransferase activity; chromatin binding; H3 histone acetyltransferase activity; histone acetyltransferase activity.
Cyclic-AMP response element binding protein B	CG6103	VDRC 101512 BDSC 29332	RNAi RNAi	DNA binding; sequence-specific DNA binding transcription factor activity; protein dimerization activity; sequence-specific DNA binding.
Myocyte enhancer factor 2	CG1429	VDRC 15550 In house	RNAi Dom neg	Metalloendopeptidase activity; DNA binding; RNA polymerase II distal enhancer or core promoter proximal region sequence-specific DNA binding transcription factor activity involved in positive regulation of transcription; sequence-specific DNA binding transcription factor activity; protein dimerization activity; enhancer sequence-specific DNA binding.
14-3-3ζ (leo)	CG17870	VDRC 104496	RNAi	Protein binding; protein domain specific binding; protein kinase C inhibitor activity; protein homodimerization activity; protein heterodimerization activity; tryptophan hydroxylase activator activity.
Smrter	CG4013	VDRC 106701	RNAi	DNA binding; chromatin binding; transcription corepressor activity; protein binding.
Lesswright (Ubc9)	CG3018	VDRC 33685 BDSC 9318	RNAi Dom neg	SUMO transferase activity; SUMO ligase activity; transcription factor binding; heat shock protein binding; ubiquitin activating enzyme binding.
Nup358 (RanBP2)	CG11856	VDRC 38583	RNAi	Zinc ion binding; Ran GTPase binding.
Sin3A	CG8815	VDRC 105852	RNAi	Sequence-specific DNA binding transcription factor activity; transcription cofactor activity; protein heterodimerization activity; chromatin binding.

CG, computed gene name; VDRC/BDSC no., catalogue number from the Vienna *Drosophila* Resource Center or the Bloomington *Drosophila* Stock Center; dom neg, dominant negative.

than by a specific genetic interaction between *HDAC4* and the RNAi-targeted gene), initial control experiments were undertaken to examine the effect of expressing a second *UAS*-driven construct on the rough eye phenotype. *UAS-HDAC4* was coexpressed with either *UAS-lacZ* or *UAS-EGFP*, and neither of them altered the *HDAC4* rough eye phenotype, confirming that the presence of a second *UAS* line does not itself alter the level of expression of *HDAC4* (Figure 1E).

A candidate screen of RNAi lines available from VDRC was performed with the purpose of identifying modifiers of the HDAC4-induced phenotype. The RNAi lines to be included in the screen were chosen by mining literature and databases such as DroID (Murali *et al.* 2011). The criteria for selection included genes known to be involved in synaptic plasticity, memory, and/or neurological functioning, other chromatin modifiers, as well as genes with identified interactions with *HDAC4* in other model systems and/or nonneuronal tissues (*e.g.*, potential pleiotropic effectors). The RNAi lines were screened by scoring the eye phenotypes that resulted from coexpression with *HDAC4*. Eyes were scored semiquantitatively on the appearance of their bristles, pigmentation, and ommatidia. The eye phenotype resulting from *GMR*-driven expression of each RNAi line was also scored and lines with more than a very mild rough eye phenotype were excluded. Sixteen genes that are already known to interact with *HDAC4* in other model systems or tissues were initially screened in order to identify interactions that are conserved between *Drosophila* and other species, as well as pleiotropic interactions in *Drosophila* (Supplemental Material, Table S1). Two genes, *smt3* (*SUMO*) and *nejire* (*Creb binding protein*), were excluded, as they caused a rough eye phenotype when knocked down with *GMR-GAL4*. Of the remaining 14 genes, 8 enhanced the *HDAC4* rough eye phenotype (Table 2), providing validation for the ability of the screen to detect interactions with *HDAC4*. These included the transcription factors *CrebB* and *Mef2*, the transcriptional corepressors *Smrter* and *Sin3A*, and the histone acetyl transferase *Gcn5*. We also observed interactions with the molecular chaperone 14-3-3ζ, the nucleoporin *Nup358 (RanBP2)*, and the E2 SUMO-conjugating enzyme *lwr* (*Ubc9*). Examples of rough eye phenotypes are shown in Figure 2, A–C. The enhancement of the rough eye phenotype when these genes are knocked down strongly suggests that these interactions are also conserved in *Drosophila*.

A further panel of 96 RNAi lines was then screened and 18 were found to enhance the *HDAC4* rough eye phenotype (Table 3). Examples of eye phenotypes from interacting genes are shown in Figure 2, D–F. Additional RNAi lines targeted to different regions of the mRNA were tested for a subset of the genes to confirm the specificity of the knockdown (Table 3). We also screened a subset of genes we identified by RNAseq, which consisted of those that were expressed significantly in the brain (as assessed by a score of >10 on FlyAtlas); however, none of these 11 genes enhanced the HDAC4 rough eye phenotype (Table S1). An in-depth functional network analysis was then performed in order to identify subsets of genes with functions in common that could be used as an aid to guide further investigation. The Search Tool for the Retrieval of Interacting Genes (STRING) database predicts physical and functional links between proteins and provides an integrated confidence score for the predicted associations (Franceschini *et al.* 2013;

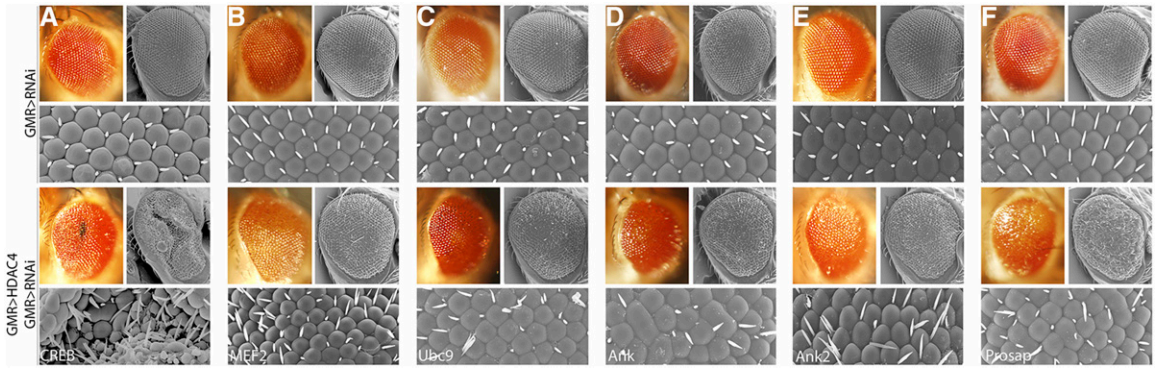

Figure 2 Enhancers of the *HDAC4* rough eye phenotype. (Top) Stereomicrographs and scanning electron micrographs of the eye phenotypes resulting from *GMR-GAL4* induced expression of the RNAi lines only. (Bottom) Phenotypes resulting from coexpression of the RNAi and *HDAC4*. The phenotype due to *GMR-GAL4*-induced expression of one copy of *HDAC4* was enhanced by coexpression of the RNAi targeted to (A) *CrebB*, (B) *MEF2*, (C) *Ankyrin*, (D) *Ankyrin 2*, (E) *Ubc9*, and (F) *Prosap*.

Szklarczyk *et al.* 2015); and furthermore, genes that represent real interactions, are more likely to connect in a network than false positives (Wang *et al.* 2009). STRING analysis of the 26 genes identified in our screen revealed potential mechanistic links between *HDAC4* and genes encoding proteins with nuclear functions (*Smr*, *Gcn5*, *Sin3A*, and *CrebB*), proteins involved in SUMOylation (*Nup358* and *Ubc9*), and proteins that interact with the cytoskeleton or influence cytoskeletal growth (*Moesin*, *Ankyrin*, *Ankyrin 2*, *Netrin-B*, *trio*, *Sra-1*, *derailed*, and *Prosap*) (Figure 3). In neurons, the latter group of genes also regulates axon and/or dendritic growth (Harris *et al.* 1996; Bonkowsky *et al.* 1999; Schenck *et al.* 2003; Lee *et al.* 2007; Briancon-Marjollet *et al.* 2008; Iyer *et al.* 2012; Siegenthaler *et al.* 2015; Yasunaga *et al.* 2015).

HDAC4 interacts with the SUMOylation machinery

We chose to initially focus on the interaction between *HDAC4* and *Ubc9*, the sole E2-conjugating enzyme in the SUMOylation pathway. SUMOylation is a process by which a small SUMO peptide is conjugated to a protein substrate (Figure 4A). It is a similar process to ubiquitination; however, rather than targeting the protein for degradation, the conjugation of SUMO alters properties of the substrate protein such as activity, stability, or subcellular localization (Wilkinson *et al.* 2010). The genes encoding the SUMOylation machinery are conserved in *Drosophila* (Long and Griffith 2000; Talamillo *et al.* 2008) and the SUMOylation machinery is enriched in fly heads (Long and Griffith 2000). SUMOylation is dependent on the presence of Ubc9 (Bhaskar *et al.* 2000), and *Ubc9* mutants display impaired SUMOylation of substrates (Miles *et al.* 2008). The genetic interaction between *HDAC4* and *Ubc9* was particularly interesting as a growing body of evidence indicates that SUMOylation is an important mechanism for regulation of neuronal protein activity (Henley *et al.* 2014) and for regulation of memory formation (Yang *et al.* 2012; Castro-Gomez *et al.* 2013; Luo *et al.* 2013; Chen *et al.* 2014; Wang *et al.* 2014; Drisaldi *et al.* 2015). Moreover, HDAC4 has also been implicated as a putative E3 SUMO ligase, as its presence enhances the SUMOylation of MEF2 (Gregoire and Yang 2005; Zhao *et al.* 2005) and of the androgen receptor (Yang *et al.* 2011) in mammalian cells. To further explore the link between *HDAC4* and SUMOylation, we investigated the interaction of *HDAC4* with *Ubc9* and other members of the SUMOylation machinery (Table 4). We found that a dominant negative mutant of *Ubc9* also enhanced the *HDAC4* eye phenotype. In addition, *Ubc9* interacted with a catalytically inactive mutant of *HDAC4*, H968A, in which a histidine residue in the active site is replaced with an alanine (Wang *et al.* 1999; Huang *et al.* 2000; Cohen *et al.* 2009; Fitzsimons *et al.* 2013), indicating that this interaction is not dependent on deacetylase activity (Table S1). *Ulp1*, the SUMO protease, also enhanced the *HDAC4* phenotype, as did the E1-conjugating enzyme *Uba2* and the E3 SUMO ligase *PIAS* (also known as *Su(var)2-10*). Notably, the nucleoporin *RanBP2*, which we identified as an *HDAC4* interactor, is also an E3 SUMO ligase. The only component of the core SUMOylation machinery that we did not detect an interaction with was the E1-conjugating enzyme subunit *Aos1*.

Although the control *GMR-GAL4* heterozygote did not have a visible eye phenotype, it has been previously reported that when driven by *GMR* at high levels, GAL4 can itself impair eye development. To validate that the phenotype was not due to an interaction with *GMR-GAL4*, we circumvented the use of *GMR-GAL4* by generating flies in which the *GMR* enhancer directly drives *HDAC4* in the eye (*GMR-HDAC4*). Additionally, expression of RNAi lines was driven by *GAL4* under control of the *eyeless* (*ey*) enhancer rather than the GMR enhancer–promoter (Hazelett *et al.* 1998). *Ey* drives expression of *GAL4* primarily anterior to the morphogenetic furrow in eye disc and *GMR*-driven expression is predominantly posterior to the furrow; however, there is some overlap (Cao *et al.* 2008). Thus in flies that carry *GMR-HDAC4*, *ey-GAL4*, and *UAS-RNAi*, only a fraction of the eye cells would coexpress *HDAC4* and *GAL4* (and the regulated RNAi). The limited coexpression would increase the chance of false negatives; however, an advantage of employing *ey-GAL4* is that since heterozygous *ey-GAL4* flies have normal eye development (Figure 4B), the temperature can

Table 3 Novel genes identified to interact with *HDAC4* in *Drosophila*

Gene name	CG no.	VDRC no.	Molecular function/biological process
krasavietz	CG2922	102609	Ribosome binding; translation initiation factor binding/axon midline choice point recognition; neuron fate commitment; positive regulation of filopodium assembly; behavioral response to ethanol; long-term memory; negative regulation of translation.
Prosap	CG30483	103592 21216	GKAP/Homer scaffold activity; postsynaptic density assembly.
rogdi	CG7725	107310	Unknown/learning or memory; behavioral response to ethanol; olfactory learning.
Ankyrin 2	CG42734	107369 40638	Cytoskeletal protein binding; structural constituent of cytoskeleton/neuromuscular junction development; short-term memory; positive regulation of synaptic growth at neuromuscular junction; negative regulation of neuromuscular synaptic transmission; axon extension.
CG5846	CG5846	107793	Unknown/unknown.
Moesin	CG10701	110654	Cytoskeletal protein binding; protein binding; actin binding; phosphatidylinositol-4,5-bisphosphate binding/actin filament-based process; sensory organ development.
Ankyrin	CG1651	25945 25946	Cytoskeletal protein binding; structural constituent of cytoskeleton/cytoskeletal anchoring at plasma membrane; signal transduction.
RanBP21	CG12234	31706	Ran GTPase binding/intracellular protein transport.
trio	CG18214	40138	Protein serine/threonine kinase activity; Rho guanyl-nucleotide exchange factor activity/actin filament-based process; regulation of neurogenesis; neuron differentiation.
Scamp	CG9195	9130	Unknown/protein transport; long-term memory; neuromuscular synaptic transmission; synaptic vesicle exocytosis.
schnurri	CG7734	105643	Sequence-specific DNA binding transcription factor activity; RNA polymerase II transcription coactivator activity/learning or memory; sensory organ development.
amnesiac	CG11937	5606	G-protein coupled receptor binding; neuropeptide hormone activity/learning or memory; associative learning; thermosensory behavior.
Imp	CG1691	20321	mRNA binding; nucleotide binding/nervous system development; mRNA splicing, via spliceosome; synaptic growth at neuromuscular junction.
Netrin-B	CG10521	100840	Unknown/motor neuron axon guidance; regulation of photoreceptor cell axon guidance; dendrite guidance; synaptic target attraction; glial cell migration; synaptic target recognition; axon guidance.
derailed	CG17348	27053	Serine-threonine/tyrosine-protein kinase/protein tyrosine kinase activity; transmembrane receptor protein tyrosine kinase activity.
crammer	CG10460	22752	Cysteine-type peptidase activity; cysteine-type endopeptidase inhibitor activity/short-term memory; inhibition of cysteine-type endopeptidase activity; long-term memory.
Sra-1	CG4931	108876	Rho GTPase binding; cell morphogenesis; axon guidance; regulation of cell shape; cell projection assembly; cortical actin cytoskeleton organization; regulation of synapse organization; cell adhesion mediated by integrin; phagocytosis; compound eye morphogenesis.
highwire	CG32592	26998	Ubiquitin-protein transferase activity; protein binding; zinc ion binding; single-organism process; regulation of synapse assembly; regulation of synaptic growth at neuromuscular junction; regulation of growth; metabolic process; response to axon injury; cellular metabolic process; regulation of metabolic process; regulation of signal transduction; cellular protein metabolic process; locomotion.

be raised to 30° to enhance GAL4 activity and therefore RNAi expression. At 30° *GMR-HDAC4* heterozygotes displayed a minimal rough eye phenotype (Figure 4C). Knockdown of the SUMO protease *Ulp1* had no effect on eye development by itself (Figure 4D), but noticeably enhanced the *GMR-HDAC4* phenotype (Figure 4E). Knockdown of *Ubc9* with *ey-GAL4* was lethal at 30°; however, at 22° there were some survivors with severely reduced eyes (Figure 4F). This was not due to an off-target effect, as the eye deficits resulting from knockdown of *Ubc9* were largely rescued by coexpression of *Ubc9* (Ubc9OE) (Figure 4H). *Ey-GAL4* driven expression of *Ubc9* alone did not appreciably affect eye development (Figure 4G). *GMR-HDAC4* heterozygotes displayed almost WT eyes at 22° (Figure 4I); however, coexpression with *Ubc9* resulted in a very severe rough eye (Figure 4J) and in some cases, complete loss of the eye (Figure 4K), indicating a genetic interaction between *HDAC4* and *Ubc9*. Similarly, knockdown of the E3 ligase *PIAS* was semilethal, with survivors displaying rough eyes that were reduced in size (Figure 4L). Coexpression of *HDAC4* resulted in a more severe phenotype with necrotic patches (Figure 4M). A summary of the HDAC4 eye phenotypes resulting from knockdown of the SUMOylation machinery genes with *GMR-GAL4* and *ey-GAL4* is provided in Table 4.

Ubc9 is required for LTM

In a proof-of-principle experiment to determine whether SUMOylation is required for LTM in *Drosophila*, we knocked down *Ubc9* panneuronally with the *elav* driver, which was confirmed by RT-qPCR (Figure S1), and assessed 24-hr memory using the courtship suppression assay. In this assay, a male fly is exposed to a freshly mated nonresponsive female and his ability to remember this rejection behavior is measured as a reduction in courtship toward subsequent females. Flies with intact memory will form a robust LTM that is stable for at least 24 hr following a 7-hr training session (Keleman *et al.* 2007; Fitzsimons and Scott 2011). Memory is calculated by dividing the CI of each male fly of the test genotype by the mean CI of the sham flies of the test genotype that received no training ($CI_{trained}/mCI_{sham}$), allowing comparison of

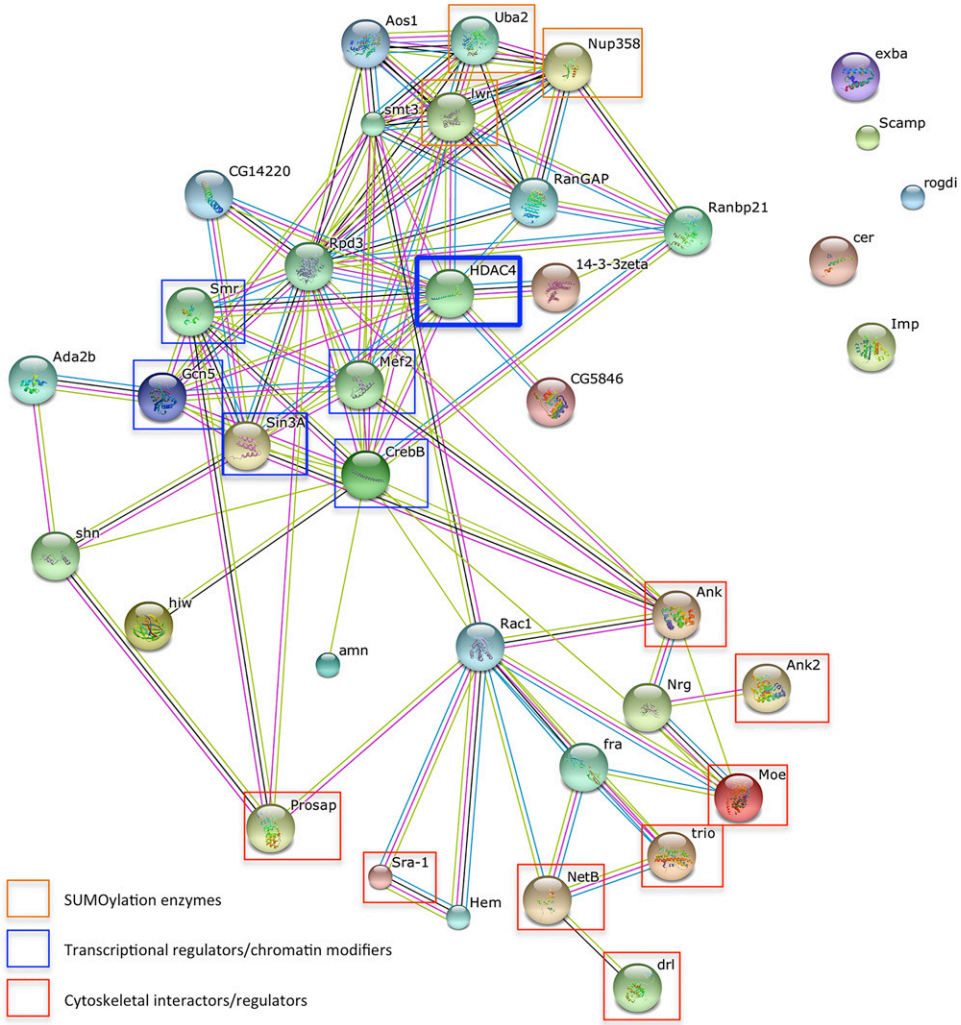

Figure 3 STRING network analysis of genes identified in the rough eye screen. Functional network analysis was performed using the STRING database, which integrates known and predicted interactions to construct and visualize protein interaction networks. Each edge represents a known or predicted interaction. Analysis of the 26 genes revealed several classes of genes that interacted with *HDAC4*. *HDAC4* is highlighted by a bold blue rectangle. Orange, blue, and red rectangles highlight genes identified in the screen that are involved in SUMOylation, chromatin modification/transcriptional regulation, and regulation of the actin cytoskeleton, respectively.

memory between genotypes (Mehren and Griffith 2004; Ejima *et al.* 2005, 2007). A score of 0 indicates the highest memory performance possible, and a score of ≥1.0 indicates performance similar to untrained sham controls. LTM was completely disrupted in flies with reduced Ubc9 (Figure 5A). Immunohistochemistry against Fasciclin II, which is expressed in the α-, β-, and γ-lobes of the mushroom body (MB) and allows visualization of the gross MB structure, did not reveal any obvious deficits in brain development; however, when we elevated the temperature from 25° to 30°, which results in higher GAL4 activity, we did observe deficits in α- and β-lobe development (Figure S1). Therefore to dissociate an effect on brain development from a specific role in the adult brain, the TARGET system was used to restrict *Ubc9* knockdown to adulthood. Flies were raised at the permissive temperature of 19°, then transferred to 30° to induce RNAi expression at 3 days posteclosion, and were trained after 48 hr at 30°. These flies were also severely impaired, with 24-hr memory scores similar to untrained controls (Figure 5B), indicating a nondevelopmental impairment in LTM. However analysis of courtship activity revealed that *Ubc9* knockdown flies also displayed a small but significant reduction in courtship activity (Figure 5C), which confounded this analysis as the decreased courtship may alter the flies' ability to form a memory. We therefore elected use of the OK107 driver to restrict *Ubc9* knockdown largely to the MB (Aso *et al.* 2009; Fitzsimons and Scott 2011). This is a critical brain region for long-term courtship memory (McBride *et al.* 1999; Keleman *et al.* 2007) but is dispensable for courtship activity (McBride *et al.* 1999). Induction of *Ubc9* knockdown in the adult MB had no effect on naïve courtship compared to controls (Figure 5E). Flies of the same genotype in which *Ubc9* RNAi was not induced (*e.g.*, raised and maintained at 19°) displayed normal LTM, whereas those in which *Ubc9* knockdown was induced in adulthood were deficient in LTM formation (Figure 5D).

HDAC4 and Ubc9 interact during LTM formation

Taken together, these data indicate that *HDAC4* interacts with the SUMOylation machinery, and depletion of the E2 SUMO-conjugating enzyme in the adult MB prevents LTM formation. Since overexpression of *HDAC4* in the MB also results in impaired LTM (Fitzsimons *et al.* 2013), we therefore sought to determine whether this interaction is important for normal

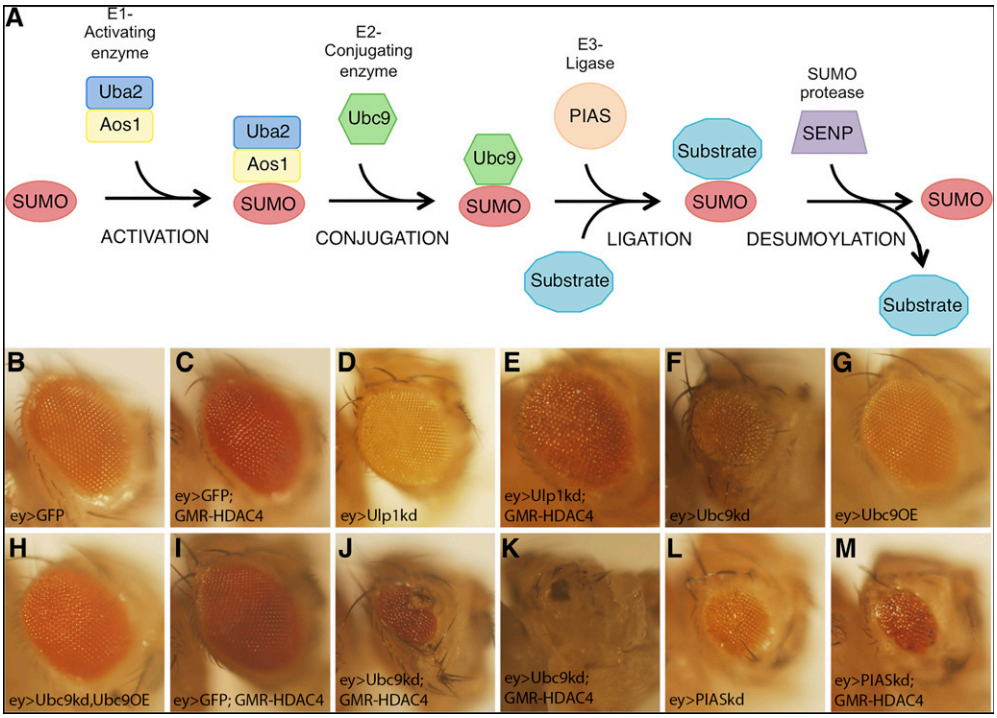

Figure 4 SUMOylation genes enhance the HDAC4 rough eye phenotype. (A) Schematic showing the process of SUMOylation and deSUMOylation of a target protein. (B–M) Stereomicrographs of *Drosophila* eyes. Flies in B–E were raised at 30° and flies in F–M were raised at 22°. (B) *Ey-GAL4*-induced expression of *GFP* does not affect eye development. (C) *GMR-HDAC4* results in a mild rough eye phenotype at 30°. (D) Knockdown of *Ulp1* has no effect on eye development. (E) Coexpression of *Ulp1* and *HDAC4* results in a severe rough eye phenotype. (F) *Ey*-induced expression of *Ubc9* RNAi results in a small rough eye. (G) Expression of *Ubc9* does not affect eye development. (H) *Ubc9* overexpression rescues the *Ubc9* RNAi eye phenotype. (I) Eyes appear normal when *GMR-HDAC4* is expressed at 25°. (J and K) Coexpression of *ey > Ubc9* and *GMR-HDAC4* enhances the *HDAC4* eye phenotype, sometimes causing complete loss of the eye. (L) Eye-driven expression of *PIAS* RNAi impairs eye development. (M) This phenotype is significantly enhanced by *GMR-HDAC4*.

memory formation. As the TARGET system is temperature sensitive, we reasoned that lowering expression of *HDAC4* and *Ubc9* RNAi by approximately half may provide a scenario in which there was insufficient expression to impair LTM, which would allow assessment of a genetic interaction between the two genes. We found that at 24°, expression of the quantitative reporter luciferase was induced to half the maximal expression obtained at 30° (Figure S2). We raised flies at 19° and then incubated individual males of each genotype at 24° for 3 days. Males expressing *Ubc9* RNAi or *HDAC4* did develop LTM although the memory indices were lower than controls (Figure 5F). Expression of both *Ubc9* RNAi and *HDAC4* together resulted in a significant impairment in memory compared to the control group (Figure 5F), and there was no significant difference in courtship activity between the groups (Figure 5G). Therefore, these data provide further evidence that *HDAC4* and *Ubc9* interact during LTM.

We next sought to determine if HDAC4 alters protein SUMOylation in *Drosophila*. In WT head extracts, high molecular weight SUMOylated proteins are observed as a smear in the presence of NEM, which inhibits the deconjugating activity of SUMO protease (Figure 6A, compare control lanes ± NEM), as previously characterized (Kanakousaki and Gibson 2012). We did not observe a global change in the abundance or molecular weights of SUMOylated conjugates following panneuronal overexpression of *HDAC4* (Figure 6A, compare control and dHDAC4 lanes). This may indicate that HDAC4 influences the SUMOylation state of a limited number of targets. Thus we next examined the impact of *HDAC4* overexpression on the SUMOylation of candidate proteins CaMKII, MEF2, and CREB, neuronal proteins that are involved in memory formation (Mehren and Griffith 2004; Barbosa *et al.* 2008; Cole *et al.* 2012; Tubon *et al.* 2013), which also have been demonstrated to interact physically with HDAC4 (Miska *et al.* 1999; McKinsey *et al.* 2000; Backs *et al.* 2008; Li *et al.* 2012), and are SUMO substrates (Long and Griffith 2000; Gregoire and Yang 2005; Zhao *et al.* 2005; Chen *et al.* 2014). However, we did not observe any species indicative of a SUMOylated form of CREB or CaMKII with standard (Figure 6B) or long exposures (Figure 6C). When probed with anti-MEF2, the samples treated with NEM did contain an additional band ~15–20 kDa larger, which could indicate a SUMOylated form (Bhaskar *et al.* 2000). However the abundance of this higher molecular weight form was not altered by overexpression of HDAC4. Given that a high proportion of SUMOylated proteins are nuclear (Hendriks *et al.* 2014), we also generated transgenic flies harboring a nuclear-restricted phosphomutant of human HDAC4 (3SA) that is unable to exit the nucleus (Grozinger and Schreiber 2000; Chawla *et al.* 2003). However, neither 3SA nor WT human HDAC4 altered the SUMOylation profile of proteins extracted from fly heads (Figure 6A). Lastly, we examined whether the interaction with the SUMOylation machinery might indicate SUMOylation of HDAC4 itself. However, following IP of HDAC4::EYFP (an internal fusion of EYFP into the endogenous HDAC4 protein) (Knowles-Barley *et al.* 2010), a SUMOylated form of HDAC4 was not detected (Figure 6D).

Table 4 Genes that encode components of the SUMOylation machinery and their effect on the *HDAC4*-induced rough eye phenotype

Gene name	Annotation symbol	VDRC/BDSC no.	Method	Molecular function	REP
Lesswright (Ubc9)	CG3018	VDRC 33685 BDSC 9318	RNAi Dom neg	SUMO ligase activity; transcription factor binding; heat shock protein binding; ubiquitin-activating enzyme binding.	E/E
Nucleoporin 358 kDa (RanBP2)	CG11856	VDRC 38583	RNAi	Zinc ion binding; Ran GTPase binding.	E/N
Ulp1	CG12359	VDRC 31744	RNAi	SUMO-specific protease activity; protein binding.	E/E
Uba2	CG7528	VDRC 110173	RNAi	SUMO-activating enzyme activity; small protein activating enzyme activity; ubiquitin-activating enzyme binding; ubiquitin-activating enzyme activity.	E/Ex
Activator of SUMO 1	CG12276	VDRC 47256	RNAi	Ubiquitin-conjugating enzyme binding; ubiquitin-activating enzyme binding; small protein activating enzyme activity; SUMO-activating enzyme activity.	N/Ex
Suppressor of variegation 2-10 (PIAS)	CG8068	VDRC 30709	RNAi	Zinc ion binding; DNA binding; DEAD/H-box RNA helicase binding.	E/E

The REP results are shown for each RNAi line tested in combination with *UAS-HDAC4*; *GMR-GAL4* and *GMR-HDAC4*; *ey-GAL4*, respectively, separated with a backslash. *Uba2* and *Aos1* were unable to be tested in the *GMR-HDAC4*; *ey-GAL4* screen as RNAi expression in combination with *GMR-HDAC4* was lethal. REP, rough eye phenotype; Dom neg, dominant negative mutant; E, enhancer of rough eye phenotype; N, no effect on rough eye phenotype; Ex, excluded.

Discussion

We sought to progress our understanding of the mechanisms through which HDAC4 regulates memory by analysis of both transcriptional changes resulting from genetic manipulation of *HDAC4* and identification of genes that interact genetically with *HDAC4*. We detected very few changes in transcription induced by overexpression of *HDAC4*; indeed the gene for which transcript abundance increased the most was *HDAC4* itself. This lack of *HDAC4*-induced transcriptional changes is consistent with recent studies in the mouse in which manipulation of WT *HDAC4* expression did not result in significant alteration of the transcriptome (Kim *et al.* 2012; Mielcarek *et al.* 2013), providing further support for the hypothesis that WT *HDAC4* has a minimal effect on transcription. An alternative explanation for the lack of transcriptional changes could be that HDAC4 does not engage with the endogenous transcriptional machinery; however, we believe this to be less likely, as we have previously shown that when overexpressed in the mushroom body, HDAC4 induces redistribution of the transcription factor MEF2 into HDAC4-positive punctate nuclear foci (Fitzsimons *et al.* 2013). The lack of transcriptional changes also does not exclude the possibility that HDAC4 regulates local changes in gene expression in a subset of nuclei that are not detectable by whole head transcriptome analyses. Indeed, a nuclear-restricted HDAC4 mutant resulted in changes in transcript abundance of a subset of genes in primary cortical neurons that was enriched for genes involved in synaptic function (Sando *et al.* 2012). Further, we found genetic interactions between *HDAC4* and known gene regulators (see below). Thus it could be worthwhile to use the INTACT technique (Deal and Henikoff 2011; Henry *et al.* 2012) to investigate *HDAC4*-dependent gene expression changes in specific neurons in the adult brain (*e.g.*, Kenyon cells). However, given the largely nonnuclear subcellular localization of both mammalian (Darcy *et al.* 2010) and *Drosophila* HDAC4 (Fitzsimons *et al.* 2013), and the impairment in memory that results from reduction of *HDAC4*, we have proposed that the presence of *HDAC4* is also required for normal memory formation through nontranscriptional mechanisms (Fitzsimons 2015). This led us to extend our search beyond differential gene expression and perform a rough eye screen to identify genes that enhance the *HDAC4*-induced rough eye phenotype.

We identified 26 genes that interacted with *HDAC4* and many of these genes could be classed into the three broad categories of transcriptional regulators/chromatin modifiers, cytoskeletal interactors/regulators, and components of the SUMOylation machinery. Several of the transcriptional regulators have previously been identified to interact with *HDAC4* in mammalian cells. A physical interaction between HDAC4 and MEF2, which results in repression of MEF2 activity, has been well documented (Miska *et al.* 1999; Wang *et al.* 1999; Lu *et al.* 2000; Fitzsimons *et al.* 2013). Similarly, HDAC4 also binds to and inhibits CREB in mouse brain (Li *et al.* 2012). We also confirmed that *HDAC4* interacts with the transcriptional corepressor *Smrter*, the *Drosophila* ortholog of human *SMRT*, which requires HDAC4 binding for its corepressor activity (Huang *et al.* 2000; Fischle *et al.* 2002). The enhancement of the *HDAC4* rough eye phenotype when these genes are knocked down strongly suggests that these interactions are also conserved in *Drosophila* neurons. We also identified putative novel interactions with transcriptional regulators *schnurri* and *rogdi*, which were both previously identified in a screen for *Drosophila* olfactory memory mutants, with transposon insertions in both of the genes resulting in severely impaired 24-hr memory, without affecting learning (Dubnau *et al.* 2003).

We also identified a number of genes encoding proteins that interact with or regulate the actin cytoskeleton, including *trio*, *Sra-1*, *Prosap*, *Netrin-B*, *krasavietz*, *Moesin*, *Ankyrin 2*, and *Ankyrin*. This is of particular interest as activity-dependent reorganization of the actin cytoskeleton occurs during growth of dendritic spines, which are thought to represent the structural changes that underpin the formation of new memories (Engert and Bonhoeffer 1999; Holtmaat and Svoboda 2009;

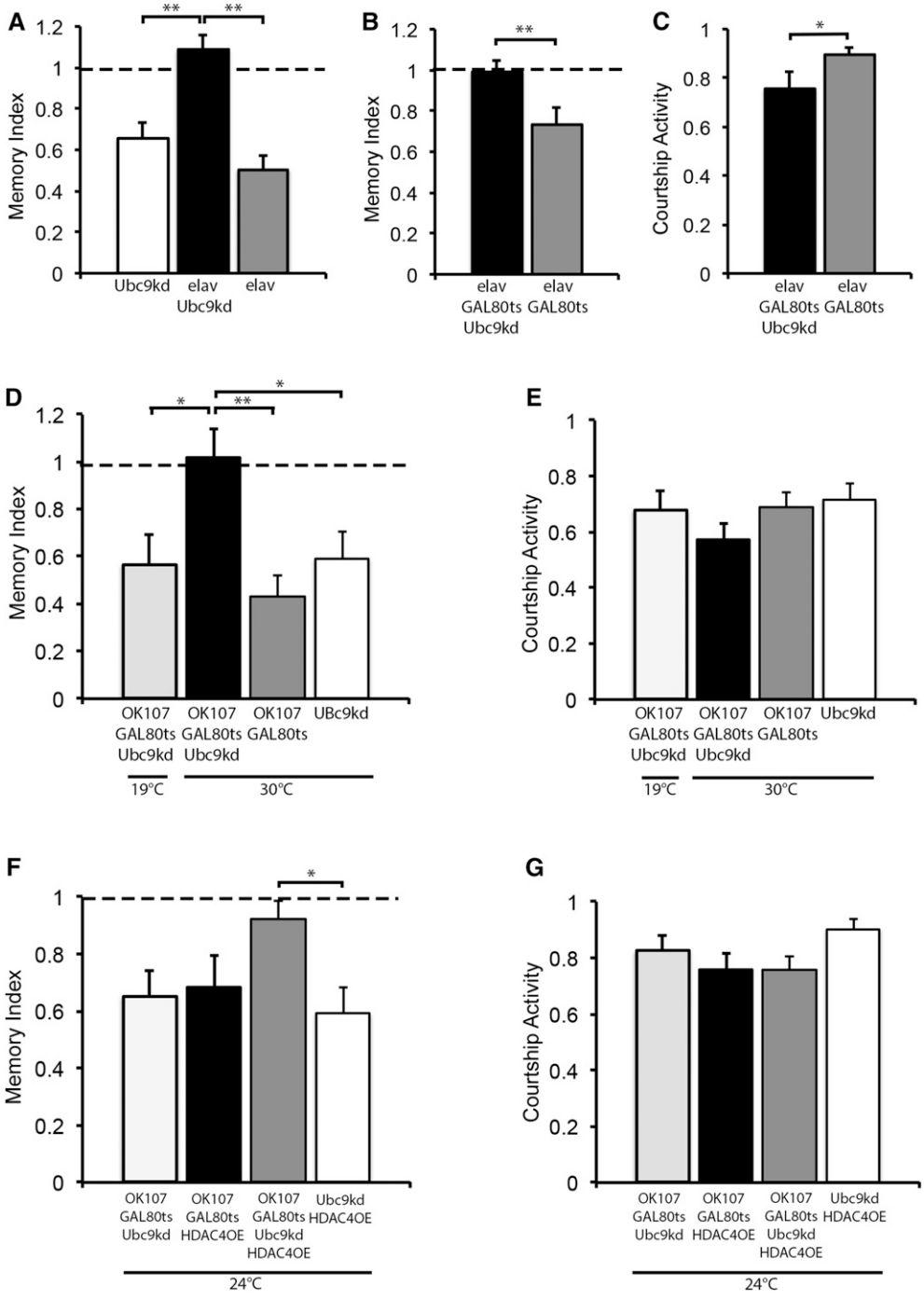

Figure 5 Knockdown of *Ubc9* impairs LTM. (A) Knockdown of *Ubc9* throughout development with *elav-GAL4* resulted in a significant impairment in 24-hr LTM compared to control genotypes (ANOVA, *post hoc* Tukey's HSD, ** $P < 0.01$). (B) Flies were raised to adulthood at 19° and switched to 30° 3 days prior to testing at 25° in order to induce expression of the *Ubc9* RNAi. Twenty-four hour LTM was significantly impaired (Student's *t*-test, two tailed, unpaired, ** $P < 0.01$). (C) There was also a significant reduction in courtship activity in these flies (Student's *t*-test, two tailed, unpaired, *$P < 0.05$). (D) Flies with *OK107-GAL4* driving *Ubc9* RNAi under control of the TARGET system had normal memory in the uninduced state (raised at 19°); however, memory was abolished when gene expression was induced at 30°. (ANOVA, *post hoc* Tukey's HSD, * $P < 0.05$, ** $P < 0.01$). (E) Courtship activity was unaffected by knockdown of *Ubc9* in the adult brain with *OK107-GAL4*. (F) Flies were raised at 19° and then incubated at 24° for 72 hr. The combination of *Ubc9* knockdown and *HDAC4* overexpression resulted in a specific impairment in LTM compared to the control (ANOVA, *post hoc* Tukey's HSD, * $P < 0.05$). (G) Courtship activity was unaffected. Full genotype abbreviations are as follows: Ubc9kd, UAS-Ubc9kd/+; elav, elav-GAL4/Y; elav Ubc9kd, elav-GAL4/Y;UAS-Ubc9kd/+; elav GAL80ts Ubc9, elav-GAL4/Y;UAS-Ubc9kd/tub-GAL80ts; elav GAL80ts, elav-GAL4/Y; tub-GAL80ts/+; OK107 GAL80ts Ubc9kd, tub-GAL80ts/UAS-Ubc9kd;OK107-GAL4/+;OK107 GAL80ts, tub-GAL80ts/+; OK107-GAL4/+; OK107 GAL80ts HDAC4OE, tub-GAL80ts/+;UAS-HDAC4OE/+; OK107-GAL4/+; and OK107 GAL80ts Ubc9kd HDAC4OE, tub-GAL80ts/UAS-Ubc9kd;UAS-HDAC4OE/+;OK107-GAL4/+.

Yang *et al.* 2009). Several of these genes including *trio* (Iyer *et al.* 2012; Shivalkar and Giniger 2012), *Netrin B* (Harris *et al.* 1996; Mitchell *et al.* 1996), *krasavietz* (Lee *et al.* 2007; Sanchez-Soriano *et al.* 2009), and *Ankyrin 2* (Siegenthaler *et al.* 2015) regulate axon and/or dendrite growth in *Drosophila*. Moreover, *krasavietz* (Dubnau *et al.* 2003) and *Ankyrin 2* (Iqbal *et al.* 2013) are also required for memory formation. Axon and dendritic growth and branching can easily be visualized and assessed in *Drosophila* (Leiss *et al.* 2009; Goossens *et al.* 2011), which will facilitate investigation of the relationships between these genes and *HDAC4*.

As HDAC4 has also been shown to modulate SUMOylation, and accumulating evidence indicates that regulation of SUMOylation is an important mechanism for synaptic plasticity, we chose to initially focus our attention on the HDAC4-Ubc9 interaction. Although SUMOylation has been most studied in the nucleus, the SUMOylation machinery also operates at extranuclear locations, including at synapses (Loriol *et al.* 2012) where it is dynamically regulated in response to synaptic activity, resulting in transient reduction of SUMOylated proteins at synaptosomes (Loriol *et al.* 2013). The list of neuronal proteins known to be SUMOylated is rapidly rising

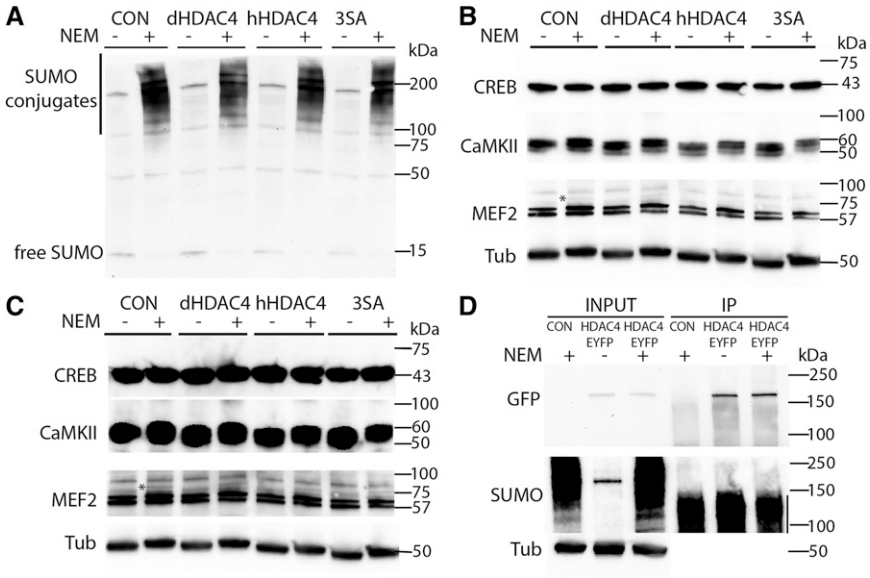

Figure 6 Assessment of SUMOylation of proteins in whole cell lysates of *Drosophila* heads. (A) Whole cell lysates were prepared from fly heads in which *elav*-driven expression of *Drosophila* HDAC4, human HDAC4, or a nuclear-restricted mutant of human HDAC4 (3SA) were induced in adulthood with the TARGET system. Lysates were prepared ± 10 mM NEM, which inhibits SUMO protease. Free SUMO is observed in the absence of NEM, whereas SUMO conjugates are observed in the presence of 10 mM NEM. There were no obvious differences in SUMOylation profiles in any of the HDAC4-overexpressing samples in comparison to the control. (B) The same samples were subjected to SDS-PAGE and probed with anti-MEF2, CaMKII, and CREB. Asterisk indicates a protein species only present in samples +NEM. Tubulin was used as a loading control. (C) Long exposure of B. (D) IP of HDAC4. Whole cell lysates from heads of HDAC4::EYFP (± 10 mM NEM) and WT control (+10 mM NEM) flies were immunoprecipitated with anti-GFP and processed for SDS-PAGE and Western blotting with the antibodies indicated on the left of the blots. Input HDAC4::EYFP samples show a band of the expected size of ~170 kDa that is not present in the control. Control and HDAC4::EYFP input samples processed with NEM display a profile of SUMOylated proteins (as seen in A). Following IP, the HDAC4::EYFP band is detected with anti-GFP; however, a product of ~190 kDa that would indicate a SUMOylated form of HDAC4::EYFP is not detected with the anti-SUMO antibody. The vertical line indicates the smear in the IP lanes, which is signal originating from the IgG heavy chain that is detected at high levels due to the very long exposure.

(Chao *et al.* 2008; Chamberlain *et al.* 2012; Cheng *et al.* 2014; for review see Henley *et al.* 2014) and this modification can have dramatic effects on function, *e.g.*, SUMOylation of an isoform of CREB resulted in increased BDNF expression in the mouse hippocampus, and was associated with enhanced spatial memory in the mouse (Chen *et al.* 2014). The prion-like cytoplasmic polyadenylation element-binding protein (CPEB3) regulates the activity-dependent translation of dormant messenger RNAs (mRNAs) at the synapse, which are required for maintenance of LTM (Kandel *et al.* 2014) and this process is regulated by SUMOylation. Formation of the insoluble prion-like form of CPEB3 is required for its activity, and this aggregation is inhibited by SUMOylation; thus when SUMOylated, CPEB3-induced translation of synaptic mRNA is inhibited and and memory formation is constrained (Drisaldi *et al.* 2015). The SUMOylation machinery is also conserved in *Drosophila* (Talamillo *et al.* 2008) and is enriched in the adult CNS where it is required for normal neuronal function (Long and Griffith 2000). Here, we have shown *Ubc9* is critically required for LTM in *Drosophila*. Moreover, nearly all components of the SUMOylation machinery interact genetically with HDAC4, suggesting the importance of SUMO for HDAC4 function. Overexpression of *HDAC4* combined with knockdown of *Ubc9* resulted in a more severe memory phenotype, suggesting an interaction between them during LTM formation. We did not observe any global changes in SUMOylation when HDAC4 was overexpressed. This was not necessarily unexpected, as E3 ligases impart substrate specificity, rather than being essential for the process of SUMOylation (Wang and Dasso 2009; Gareau and Lima 2010), and as yet, very few putative HDAC4 substrates have been identified. Also, functionally important HDAC4-mediated changes in SUMOylation could be restricted to localized regions of brain and subsets of proteins that interact with HDAC4. We were unable to detect changes in SUMOylation of candidate proteins MEF2, CaMKII, or CREB. More than 100 proteins in *Drosophila* have been identified to bind SUMO (Lehembre *et al.* 2000; Sahota *et al.* 2009; Abed *et al.* 2011; Guruharsha *et al.* 2011; Handu *et al.* 2015) and further investigation of these and other SUMOylated proteins that are involved in synaptic plasticity in other organisms may shed light on the nature of this interaction. It also should be considered that the interaction between *HDAC4* and *Ubc9* could be independent of SUMOylation. Indeed, there are a few studies in which a SUMOylation-independent role for Ubc9 has been reported, which include modulation of invasion and metastasis in a breast cancer cell line (Zhu *et al.* 2010), regulation of insulin sensitivity of glucose transport (Liu *et al.* 2007), and transcriptional activation of PLAGL2 (Guo *et al.* 2008). The specific mechanisms through which Ubc9 acts were not determined except for the latter report, in which it displayed transcriptional coactivator activity.

In summary, our findings that *HDAC4* interacts with several components of the SUMOylation machinery in *Drosophila*, and that *Ubc9* is required for LTM formation in *Drosophila*, suggest that this would be an informative model to further investigate these interactions.

Acknowledgments

We thank Niki Murray and the Manawatu Microscopy and Imaging Center, (Massey University, Palmerston North, New Zealand), for scanning electron microscopy; David Wheeler for bioinformatics advice; Elizabeth Scholl for bioinformatic

analyses; and Albert Courey and Bruce Paterson for kind gifts of the SUMO and MEF2 antibodies. We also thank New Zealand Genomics Limited for providing the bioIT platform. This work was supported by a Health Research Council of New Zealand Sir Charles Hercus Health Research fellowship and a Palmerston North Medical Research Foundation grant to H.L.F.

Literature Cited

Abed, M., K. C. Barry, D. Kenyagin, B. Koltun, T. M. Phippen *et al.*, 2011 Degringolade, a SUMO-targeted ubiquitin ligase, inhibits Hairy/Groucho-mediated repression. EMBO J. 30: 1289–1301.

Anderson, J., R. Bhandari, and J. P. Kumar, 2005 A genetic screen identifies putative targets and binding partners of CREB-binding protein in the developing Drosophila eye. Genetics 171: 1655–1672.

Andzelm, M. M., T. J. Cherry, D. A. Harmin, A. C. Boeke, C. Lee *et al.*, 2015 MEF2D drives photoreceptor development through a genome-wide competition for tissue-specific enhancers. Neuron 86: 247–263.

Aso, Y., K. Grubel, S. Busch, A. B. Friedrich, I. Siwanowicz *et al.*, 2009 The mushroom body of adult Drosophila characterized by GAL4 drivers. J. Neurogenet. 23: 156–172.

Backs, J., T. Backs, S. Bezprozvannaya, T. A. McKinsey, and E. N. Olson, 2008 Histone deacetylase 5 acquires calcium/calmodulin-dependent kinase II responsiveness by oligomerization with histone deacetylase 4. Mol. Cell. Biol. 28: 3437–3445.

Barbosa, A. C., M. S. Kim, M. Ertunc, M. Adachi, E. D. Nelson *et al.*, 2008 MEF2C, a transcription factor that facilitates learning and memory by negative regulation of synapse numbers and function. Proc. Natl. Acad. Sci. USA 105: 9391–9396.

Bhaskar, V., S. A. Valentine, and A. J. Courey, 2000 A functional interaction between dorsal and components of the Smt3 conjugation machinery. J. Biol. Chem. 275: 4033–4040.

Bonkowsky, J. L., S. Yoshikawa, D. D. O'Keefe, A. L. Scully, and J. B. Thomas, 1999 Axon routing across the midline controlled by the Drosophila Derailed receptor. Nature 402: 540–544.

Briancon-Marjollet, A., A. Ghogha, H. Nawabi, I. Triki, C. Auziol *et al.*, 2008 Trio mediates netrin-1-induced Rac1 activation in axon outgrowth and guidance. Mol. Cell. Biol. 28: 2314–2323.

Cao, W., H. J. Song, T. Gangi, A. Kelkar, I. Antani *et al.*, 2008 Identification of novel genes that modify phenotypes induced by Alzheimer's beta-amyloid overexpression in Drosophila. Genetics 178: 1457–1471.

Castro-Gomez, S., A. Barrera-Ocampo, G. Machado-Rodriguez, J. F. Castro-Alvarez, M. Glatzel *et al.*, 2013 Specific de-SUMOylation triggered by acquisition of spatial learning is related to epigenetic changes in the rat hippocampus. Neuroreport 24: 976–981.

Chamberlain, S. E., I. M. Gonzalez-Gonzalez, K. A. Wilkinson, F. A. Konopacki, S. Kantamneni *et al.*, 2012 SUMOylation and phosphorylation of GluK2 regulate kainate receptor trafficking and synaptic plasticity. Nat. Neurosci. 15: 845–852.

Chao, H. W., C. J. Hong, T. N. Huang, Y. L. Lin, and Y. P. Hsueh, 2008 SUMOylation of the MAGUK protein CASK regulates dendritic spinogenesis. J. Cell Biol. 182: 141–155.

Chawla, S., P. Vanhoutte, F. J. Arnold, C. L. Huang, and H. Bading, 2003 Neuronal activity-dependent nucleocytoplasmic shuttling of HDAC4 and HDAC5. J. Neurochem. 85: 151–159.

Chen, B., and C. L. Cepko, 2009 HDAC4 regulates neuronal survival in normal and diseased retinas. Science 323: 256–259.

Chen, Y. C., W. L. Hsu, Y. L. Ma, D. J. Tai, and E. H. Lee, 2014 CREB SUMOylation by the E3 ligase PIAS1 enhances spatial memory. J. Neurosci. 34: 9574–9589.

Cheng, J., M. Huang, Y. Zhu, Y. J. Xin, Y. K. Zhao *et al.*, 2014 SUMOylation of MeCP2 is essential for transcriptional repression and hippocampal synapse development. J. Neurochem. 128: 798–806.

Cohen, T. J., T. Barrientos, Z. C. Hartman, S. M. Garvey, G. A. Cox *et al.*, 2009 The deacetylase HDAC4 controls myocyte enhancing factor-2-dependent structural gene expression in response to neural activity. FASEB J. 23: 99–106.

Cole, C. J., V. Mercaldo, L. Restivo, A. P. Yiu, M. J. Sekeres *et al.*, 2012 MEF2 negatively regulates learning-induced structural plasticity and memory formation. Nat. Neurosci. 15: 1255–1264.

Darcy, M. J., K. Calvin, K. Cavnar, and C. C. Ouimet, 2010 Regional and subcellular distribution of HDAC4 in mouse brain. J. Comp. Neurol. 518: 722–740.

Deal, R. B., and S. Henikoff, 2011 The INTACT method for cell type-specific gene expression and chromatin profiling in Arabidopsis thaliana. Nat. Protoc. 6: 56–68.

Drisaldi, B., L. Colnaghi, L. Fioriti, N. Rao, C. Myers *et al.*, 2015 SUMOylation is an inhibitory constraint that regulates the prion-like aggregation and activity of CPEB3. Cell Reports 11: 1694–1702.

Dubnau, J., A. S. Chiang, L. Grady, J. Barditch, S. Gossweiler *et al.*, 2003 The staufen/pumilio pathway is involved in Drosophila long-term memory. Curr. Biol. 13: 286–296.

Ejima, A., B. P. Smith, C. Lucas, J. D. Levine, and L. C. Griffith, 2005 Sequential learning of pheromonal cues modulates memory consolidation in trainer-specific associative courtship conditioning. Curr. Biol. 15: 194–206.

Ejima, A., B. P. Smith, C. Lucas, W. van der Goes van Naters, C. J. Miller *et al.*, 2007 Generalization of courtship learning in Drosophila is mediated by cis-vaccenyl acetate. Curr. Biol. 17: 599–605.

Engert, F., and T. Bonhoeffer, 1999 Dendritic spine changes associated with hippocampal long-term synaptic plasticity. Nature 399: 66–70.

Fischle, W., F. Dequiedt, M. J. Hendzel, M. G. Guenther, M. A. Lazar *et al.*, 2002 Enzymatic activity associated with class II HDACs is dependent on a multiprotein complex containing HDAC3 and SMRT/N-CoR. Mol. Cell 9: 45–57.

Fitzsimons, H. L., 2015 The Class IIa histone deacetylase HDAC4 and neuronal function: Nuclear nuisance and cytoplasmic stalwart? Neurobiol. Learn. Mem. 123: 149–158.

Fitzsimons, H. L., and M. J. Scott, 2011 Genetic modulation of Rpd3 expression impairs long-term courtship memory in Drosophila. PLoS One 6: e29171.

Fitzsimons, H. L., S. Schwartz, F. M. Given, and M. J. Scott, 2013 The histone deacetylase HDAC4 regulates long-term memory in Drosophila. PLoS One 8: e83903.

Flavell, S. W., C. W. Cowan, T. K. Kim, P. L. Greer, Y. Lin *et al.*, 2006 Activity-dependent regulation of MEF2 transcription factors suppresses excitatory synapse number. Science 311: 1008–1012.

Franceschini, A., D. Szklarczyk, S. Frankild, M. Kuhn, M. Simonovic *et al.*, 2013 STRING v9.1: protein-protein interaction networks, with increased coverage and integration. Nucleic Acids Res. 41: D808–D815.

Freeman, M., 1996 Reiterative use of the EGF receptor triggers differentiation of all cell types in the Drosophila eye. Cell 87: 651–660.

Gareau, J. R., and C. D. Lima, 2010 The SUMO pathway: emerging mechanisms that shape specificity, conjugation and recognition. Nat. Rev. Mol. Cell Biol. 11: 861–871.

Goossens, T., Y. Y. Kang, G. Wuytens, P. Zimmermann, Z. Callaerts-Vegh *et al.*, 2011 The Drosophila L1CAM homolog Neuroglian signals through distinct pathways to control different aspects of mushroom body axon development. Development 138: 1595–1605.

Gregoire, S., and X. J. Yang, 2005 Association with class IIa histone deacetylases upregulates the sumoylation of MEF2 transcription factors. Mol. Cell. Biol. 25: 2273–2287.
Grozinger, C. M., and S. L. Schreiber, 2000 Regulation of histone deacetylase 4 and 5 and transcriptional activity by 14–3-3-dependent cellular localization. Proc. Natl. Acad. Sci. USA 97: 7835–7840.
Guo, Y., M. C. Yang, J. C. Weissler, and Y. S. Yang, 2008 Modulation of PLAGL2 transactivation activity by Ubc9 co-activation not SUMOylation. Biochem. Biophys. Res. Commun. 374: 570–575.
Guruharsha, K. G., J. F. Rual, B. Zhai, J. Mintseris, P. Vaidya *et al.*, 2011 A protein complex network of Drosophila melanogaster. Cell 147: 690–703.
Handu, M., B. Kaduskar, R. Ravindranathan, A. Soory, R. Giri *et al.*, 2015 SUMO-enriched proteome for Drosophila innate immune response. G3 (Bethesda) 5: 2137–2154.
Harris, R., L. M. Sabatelli, and M. A. Seeger, 1996 Guidance cues at the Drosophila CNS midline: identification and characterization of two Drosophila Netrin/UNC-6 homologs. Neuron 17: 217–228.
Hazelett, D. J., M. Bourouis, U. Walldorf, and J. E. Treisman, 1998 decapentaplegic and wingless are regulated by eyes absent and eyegone and interact to direct the pattern of retinal differentiation in the eye disc. Development 125: 3741–3751.
Hendriks, I. A., R. C. D'Souza, B. Yang, M. Verlaan-de Vries, M. Mann *et al.*, 2014 Uncovering global SUMOylation signaling networks in a site-specific manner. Nat. Struct. Mol. Biol. 21: 927–936.
Henley, J. M., T. J. Craig, and K. A. Wilkinson, 2014 Neuronal SUMOylation: mechanisms, physiology, and roles in neuronal dysfunction. Physiol. Rev. 94: 1249–1285.
Henry, G. L., F. P. Davis, S. Picard, and S. R. Eddy, 2012 Cell type-specific genomics of Drosophila neurons. Nucleic Acids Res. 40: 9691–9704.
Holtmaat, A., and K. Svoboda, 2009 Experience-dependent structural synaptic plasticity in the mammalian brain. Nat. Rev. Neurosci. 10: 647–658.
Huang, E. Y., J. Zhang, E. A. Miska, M. G. Guenther, T. Kouzarides *et al.*, 2000 Nuclear receptor corepressors partner with class II histone deacetylases in a Sin3-independent repression pathway. Genes Dev. 14: 45–54.
Iqbal, Z., G. Vandeweyer, M. van der Voet, A. M. Waryah, M. Y. Zahoor *et al.*, 2013 Homozygous and heterozygous disruptions of ANK3: at the crossroads of neurodevelopmental and psychiatric disorders. Hum. Mol. Genet. 22: 1960–1970.
Iyer, S. C., D. Wang, E. P. Iyer, S. A. Trunnell, R. Meduri *et al.*, 2012 The RhoGEF trio functions in sculpting class specific dendrite morphogenesis in Drosophila sensory neurons. PLoS One 7: e33634.
Kanakousaki, K., and M. C. Gibson, 2012 A differential requirement for SUMOylation in proliferating and non-proliferating cells during Drosophila development. Development 139: 2751–2762.
Kandel, E. R., Y. Dudai, and M. R. Mayford, 2014 The molecular and systems biology of memory. Cell 157: 163–186.
Kaplow, M. E., L. J. Mannava, A. C. Pimentel, H. A. Fermin, V. J. Hyatt *et al.*, 2007 A genetic modifier screen identifies multiple genes that interact with Drosophila Rap/Fzr and suggests novel cellular roles. J. Neurogenet. 21: 105–151.
Keleman, K., S. Kruttner, M. Alenius, and B. J. Dickson, 2007 Function of the Drosophila CPEB protein Orb2 in long-term courtship memory. Nat. Neurosci. 10: 1587–1593.
Kim, M. S., M. W. Akhtar, M. Adachi, M. Mahgoub, R. Bassel-Duby *et al.*, 2012 An essential role for histone deacetylase 4 in synaptic plasticity and memory formation. J. Neurosci. 32: 10879–10886.
Kim, Y. I., T. Ryu, J. Lee, Y. S. Heo, J. Ahnn *et al.*, 2010 A genetic screen for modifiers of Drosophila caspase Dcp-1 reveals caspase involvement in autophagy and novel caspase-related genes. BMC Cell Biol. 11: 9.
Knowles-Barley, S., M. Longair and J. D. Armstrong, 2010 BrainTrap: a database of 3D protein expression patterns in the Drosophila brain. Database (Oxford) 2010: baq005.
Kockel, L., G. Vorbruggen, H. Jackle, M. Mlodzik, and D. Bohmann, 1997 Requirement for Drosophila 14–3-3 zeta in Raf-dependent photoreceptor development. Genes Dev. 11: 1140–1147.
Kumar, A., K. H. Choi, W. Renthal, N. M. Tsankova, D. E. Theobald *et al.*, 2005 Chromatin remodeling is a key mechanism underlying cocaine-induced plasticity in striatum. Neuron 48: 303–314.
Lee, S., M. Nahm, M. Lee, M. Kwon, E. Kim *et al.*, 2007 The F-actin-microtubule crosslinker Shot is a platform for Krasavietz-mediated translational regulation of midline axon repulsion. Development 134: 1767–1777.
Lehembre, F., P. Badenhorst, S. Muller, A. Travers, F. Schweisguth *et al.*, 2000 Covalent modification of the transcriptional repressor tramtrack by the ubiquitin-related protein Smt3 in Drosophila flies. Mol. Cell. Biol. 20: 1072–1082.
Leiss, F., E. Koper, I. Hein, W. Fouquet, J. Lindner *et al.*, 2009 Characterization of dendritic spines in the Drosophila central nervous system. Dev. Neurobiol. 69: 221–234.
Li, J., J. Chen, C. L. Ricupero, R. P. Hart, M. S. Schwartz *et al.*, 2012 Nuclear accumulation of HDAC4 in ATM deficiency promotes neurodegeneration in ataxia telangiectasia. Nat. Med. 18: 783–790.
Lilly, B., B. Zhao, G. Ranganayakulu, B. M. Paterson, R. A. Schulz *et al.*, 1995 Requirement of MADS domain transcription factor D-MEF2 for muscle formation in Drosophila. Science 267: 688–693.
Liu, L. B., W. Omata, I. Kojima, and H. Shibata, 2007 The SUMO conjugating enzyme Ubc9 is a regulator of GLUT4 turnover and targeting to the insulin-responsive storage compartment in 3T3–L1 adipocytes. Diabetes 56: 1977–1985.
Long, X., and L. C. Griffith, 2000 Identification and characterization of a SUMO-1 conjugation system that modifies neuronal calcium/calmodulin-dependent protein kinase II in Drosophila melanogaster. J. Biol. Chem. 275: 40765–40776.
Loriol, C., J. Parisot, G. Poupon, C. Gwizdek, and S. Martin, 2012 Developmental regulation and spatiotemporal redistribution of the sumoylation machinery in the rat central nervous system. PLoS One 7: e33757.
Loriol, C., A. Khayachi, G. Poupon, C. Gwizdek and S. Martin, 2013 Activity-dependent regulation of the sumoylation machinery in rat hippocampal neurons. Biol. Cell 105: 30–45.
Lu, J., T. A. McKinsey, R. L. Nicol, and E. N. Olson, 2000 Signal-dependent activation of the MEF2 transcription factor by dissociation from histone deacetylases. Proc. Natl. Acad. Sci. USA 97: 4070–4075.
Luo, J., E. Ashikaga, P. P. Rubin, M. J. Heimann, K. L. Hildick *et al.*, 2013 Receptor trafficking and the regulation of synaptic plasticity by SUMO. Neuromolecular Med. 15: 692–706.
Mattaliano, M. D., E. S. Montana, K. M. Parisky, J. T. Littleton, and L. C. Griffith, 2007 The Drosophila ARC homolog regulates behavioral responses to starvation. Mol. Cell. Neurosci. 36: 211–221.
McBride, S. M., G. Giuliani, C. Choi, P. Krause, D. Correale *et al.*, 1999 Mushroom body ablation impairs short-term memory and long-term memory of courtship conditioning in Drosophila melanogaster. Neuron 24: 967–977.
McGuire, S. E., Z. Mao, and R. L. Davis, 2004 Spatiotemporal gene expression targeting with the TARGET and gene-switch systems in Drosophila. Sci. STKE 2004: pl6.

McKinsey, T. A., C. L. Zhang, J. Lu, and E. N. Olson, 2000 Signal-dependent nuclear export of a histone deacetylase regulates muscle differentiation. Nature 408: 106–111.

Mehren, J. E., and L. C. Griffith, 2004 Calcium-independent calcium/calmodulin-dependent protein kinase II in the adult Drosophila CNS enhances the training of pheromonal cues. J. Neurosci. 24: 10584–10593.

Mielcarek, M., T. Seredenina, M. P. Stokes, G. F. Osborne, C. Landles *et al.*, 2013 HDAC4 does not act as a protein deacetylase in the postnatal murine brain in vivo. PLoS One 8: e80849.

Miles, W. O., E. Jaffray, S. G. Campbell, S. Takeda, L. J. Bayston *et al.*, 2008 Medea SUMOylation restricts the signaling range of the Dpp morphogen in the Drosophila embryo. Genes Dev. 22: 2578–2590.

Miska, E. A., C. Karlsson, E. Langley, S. J. Nielsen, J. Pines *et al.*, 1999 HDAC4 deacetylase associates with and represses the MEF2 transcription factor. EMBO J. 18: 5099–5107.

Mitchell, K. J., J. L. Doyle, T. Serafini, T. E. Kennedy, M. Tessier-Lavigne *et al.*, 1996 Genetic analysis of Netrin genes in Drosophila: Netrins guide CNS commissural axons and peripheral motor axons. Neuron 17: 203–215.

Morris, B., C. Etoubleau, S. Bourthoumieu, S. Reynaud-Perrine, C. Laroche *et al.*, 2012 Dose dependent expression of HDAC4 causes variable expressivity in a novel inherited case of brachydactyly mental retardation syndrome. Am. J. Med. Genet. A. 158A: 2015–2020.

Mortazavi, A., B. A. Williams, K. McCue, L. Schaeffer, and B. Wold, 2008 Mapping and quantifying mammalian transcriptomes by RNA-Seq. Nat. Methods 5: 621–628.

Murali, T., S. Pacifico, J. Yu, S. Guest, G. G. Roberts, 3rd *et al.*, 2011 DroID 2011: a comprehensive, integrated resource for protein, transcription factor, RNA and gene interactions for Drosophila. Nucleic Acids Res. 39: D736–D743.

Robinow, S., and K. White, 1991 Characterization and spatial distribution of the ELAV protein during Drosophila melanogaster development. J. Neurobiol. 22: 443–461.

Roy, S., J. Ernst, P. V. Kharchenko, P. Kheradpour, N. Negre *et al.*, 2010 Identification of functional elements and regulatory circuits by Drosophila modENCODE. Science 330: 1787–1797.

Sahota, V. K., B. F. Grau, A. Mansilla, and A. Ferrus, 2009 Troponin I and Tropomyosin regulate chromosomal stability and cell polarity. J. Cell Sci. 122: 2623–2631.

Sanchez-Soriano, N., M. Travis, F. Dajas-Bailador, C. Goncalves-Pimentel, A. J. Whitmarsh *et al.*, 2009 Mouse ACF7 and drosophila short stop modulate filopodia formation and microtubule organisation during neuronal growth. J. Cell Sci. 122: 2534–2542.

Sando, 3rd, R., N. Gounko, S. Pieraut, L. Liao, J. Yates, 3rd *et al.*, 2012 HDAC4 governs a transcriptional program essential for synaptic plasticity and memory. Cell 151: 821–834.

Sarkar, A., P. Chachra, P. Kennedy, C. J. Pena, L. A. Desouza *et al.*, 2014 Hippocampal HDAC4 contributes to postnatal fluoxetine-evoked depression-like behavior. Neuropsychopharmacology 39: 2221–2232.

Schenck, A., B. Bardoni, C. Langmann, N. Harden, J. L. Mandel *et al.*, 2003 CYFIP/Sra-1 controls neuronal connectivity in Drosophila and links the Rac1 GTPase pathway to the fragile X protein. Neuron 38: 887–898.

Shivalkar, M., and E. Giniger, 2012 Control of dendritic morphogenesis by Trio in Drosophila melanogaster. PLoS One 7: e33737.

Siegenthaler, D., E. M. Enneking, E. Moreno, and J. Pielage, 2015 L1CAM/Neuroglian controls the axon-axon interactions establishing layered and lobular mushroom body architecture. J. Cell Biol. 208: 1003–1018.

Smith, M., V. Bhaskar, J. Fernandez, and A. J. Courey, 2004 Drosophila Ulp1, a nuclear pore-associated SUMO protease, prevents accumulation of cytoplasmic SUMO conjugates. J. Biol. Chem. 279: 43805–43814.

Szklarczyk, D., A. Franceschini, S. Wyder, K. Forslund, D. Heller *et al.*, 2015 STRING v10: protein-protein interaction networks, integrated over the tree of life. Nucleic Acids Res. 43: D447–D452.

Talamillo, A., J. Sanchez, and R. Barrio, 2008 Functional analysis of the SUMOylation pathway in Drosophila. Biochem. Soc. Trans. 36: 868–873.

Trapnell, C., A. Roberts, L. Goff, G. Pertea, D. Kim *et al.*, 2012 Differential gene and transcript expression analysis of RNA-seq experiments with TopHat and Cufflinks. Nat. Protoc. 7: 562–578.

Tubon, Jr., T. C., J. Zhang, E. L. Friedman, H. Jin, E. D. Gonzales *et al.*, 2013 dCREB2-mediated enhancement of memory formation. J. Neurosci. 33: 7475–7487.

Villavicencio-Lorini, P., E. Klopocki, M. Trimborn, R. Koll, S. Mundlos *et al.*, 2013 Phenotypic variant of Brachydactyly-mental retardation syndrome in a family with an inherited interstitial 2q37.3 microdeletion including HDAC4. European journal of human genetics. Eur. J. Hum. Genet. 21: 743–748.

Wang, A. H., N. R. Bertos, M. Vezmar, N. Pelletier, M. Crosato *et al.*, 1999 HDAC4, a human histone deacetylase related to yeast HDA1, is a transcriptional corepressor. Mol. Cell. Biol. 19: 7816–7827.

Wang, L., Z. Tu, and F. Sun, 2009 A network-based integrative approach to prioritize reliable hits from multiple genome-wide RNAi screens in Drosophila. BMC Genomics 10: 220.

Wang, L., R. M. Rodriguiz, W. C. Wetsel, H. Sheng, S. Zhao *et al.*, 2014 Neuron-specific Sumo1–3 knockdown in mice impairs episodic and fear memories. Journal of psychiatry & neuroscience. J. Psychiatry Neurosci. 39: 259–266.

Wang, Y., and M. Dasso, 2009 SUMOylation and deSUMOylation at a glance. J. Cell Sci. 122: 4249–4252.

Wilkinson, K. A., Y. Nakamura, and J. M. Henley, 2010 Targets and consequences of protein SUMOylation in neurons. Brain Res. Brain Res. Rev. 64: 195–212.

Williams, S. R., M. A. Aldred, V. M. Der Kaloustian, F. Halal, G. Gowans *et al.*, 2010 Haploinsufficiency of HDAC4 causes brachydactyly mental retardation syndrome, with brachydactyly type E, developmental delays, and behavioral problems. Am. J. Hum. Genet. 87: 219–228.

Winbush, A., D. Reed, P. L. Chang, S. V. Nuzhdin, L. C. Lyons *et al.*, 2012 Identification of gene expression changes associated with long-term memory of courtship rejection in Drosophila males. G3 (Bethesda) 2: 1437–1445.

Yang, G., F. Pan, and W. B. Gan, 2009 Stably maintained dendritic spines are associated with lifelong memories. Nature 462: 920–924.

Yang, Q. G., F. Wang, Q. Zhang, W. R. Xu, Y. P. Chen *et al.*, 2012 Correlation of increased hippocampal Sumo3 with spatial learning ability in old C57BL/6 mice. Neurosci. Lett. 518: 75–79.

Yang, Y., A. K. Tse, P. Li, Q. Ma, S. Xiang *et al.*, 2011 Inhibition of androgen receptor activity by histone deacetylase 4 through receptor SUMOylation. Oncogene 30: 2207–2218.

Yasunaga, K., A. Tezuka, N. Ishikawa, Y. Dairyo, K. Togashi *et al.*, 2015 Adult Drosophila sensory neurons specify dendritic territories independently of dendritic contacts through the Wnt5-Drl signaling pathway. Genes Dev. 29: 1763–1775.

Zhao, X., T. Sternsdorf, T. A. Bolger, R. M. Evans, and T. P. Yao, 2005 Regulation of MEF2 by histone deacetylase 4- and SIRT1 deacetylase-mediated lysine modifications. Mol. Cell. Biol. 25: 8456–8464.

Zhu, S., M. Sachdeva, F. Wu, Z. Lu, and Y. Y. Mo, 2010 Ubc9 promotes breast cell invasion and metastasis in a sumoylation-independent manner. Oncogene 29: 1763–1772.

Communicating editor: M. F. Wolfner

GENETICS

Supporting Information
www.genetics.org/lookup/suppl/doi:10.1534/genetics.115.183194/-/DC1

Long-Term Memory in *Drosophila* Is Influenced by Histone Deacetylase HDAC4 Interacting with SUMO-Conjugating Enzyme Ubc9

Silvia Schwartz, Mauro Truglio, Maxwell J. Scott, and Helen L. Fitzsimons

DOI: 10.1534/genetics.115.183194

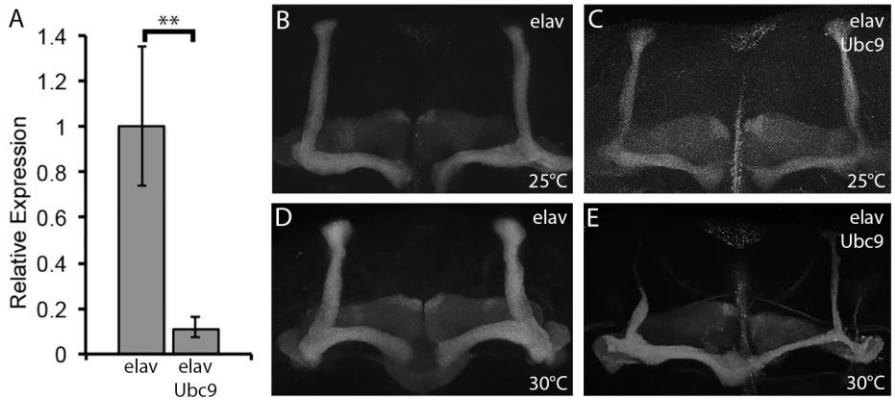

Supplementary Figure 1. Knockdown of *Ubc9* induces developmental deficits in the MB. A. RT-qPCR analysis of *Ubc9* expression. *Ubc9* RNAi was expressed pan-neuronally with elav-GAL4, followed by isolation of total RNA and RT-qPCR analysis of *Ubc9* transcript levels. *Ubc9* expression was significantly reduced in the presence of *Ubc9* RNAi. Mann-Whitney U test, **p<0.01. B,C Knockdown of *Ubc9* in flies raised at 25 °C did not appreciably affect MB development. C,D Knockdown of *Ubc9* in flies raised at 30 °C resulted in impaired α and β lobe development. Genotypes: elav = *elav-GAL4/+;* elav Ubc9 = *elav-GAL4/+;Ubc9RNAi/+*.

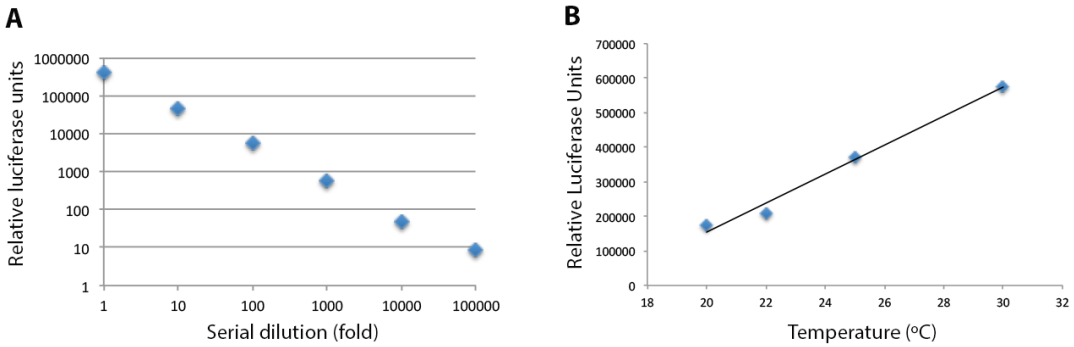

Supplementary Figure 2. Luciferase assay measuring relative GAL4 activity under GAL80ts control at different temperatures. A. Standard Curve of luciferase activity showing linearity of the assay. Serial 10-fold dilutions of Drosophila head lysate from *elav-GAL4/+; UAS-luciferase/+* flies were assayed for luciferase activity. B. Flies of the genotype *tub-GAL80ts/+; UAS-luciferase/+;OK107-GAL4/+* were incubated for 2 days at 20, 22, 25 and 30 ºC. Heads were homogenized in 1x Reporter lysis buffer, then 2 µl of lysate was used in the luciferase assay. All samples were tested in triplicate.

TABLE S1. GENES TESTED IN THE ROUGH EYE PHENOTYPE SCREEN

Gene Symbol	Flybase ID	VDRC ID	Biological function	REP
Gcn5	CG4107	21786	Histone acetyltransferase	E
CrebB	CG6103	101512 29332 (BDSC)	cAMP dependent transcriptor factor	E E
14-3-3ζ	CG17870	104496	Phosphoserine/theorine interacting protein	E
Sin3A	CG8815	105852	Transcription cofactor	E
Smr	CG4013	106701	Transcriptional corepressor	E
Nup358	CG11856	38583	Zinc ion binding protein, Ran binding protein	E
Mef2	CG1429	15550 Dom neg (in house)	Transcription factor	E E
lwr	CG3018	33685 9318 (BDSC) Dom neg	SUMO E2-conjugating enzyme	E E E
Hdac3	CG2128	20814	Histone deacetylase	N
dCaMKII	CG18069	100265	Ca^{2+}/Calmodulin-dependent protein kinase	N
Emb	CG13387	103767	Exportin	N
foxo	CG3143	106097	Transcription factor	N
sima	CG7951	106187	Transcription factor	N
nej	CG15319	105115	CBP binding protein, histone acetyltransferase	EX
Smt3	CG4494	105890	SUMO	EX
Rpd3	CG7471	30600	Histone deacetylase	N
kek2	CG4977	4745	Unknown	N
CAH	CG6906	8357	Carbonate dehydratase	N
lanA	C10236	18873	Receptor binding protein	N
Arc1	CG12505	31122	Nucleic acid binding protein	N
CG9377	CG9377	42835	Unknown	N
Odp56b	CG11218	100671	Odorant binding protein	N
CG6409	CG6409	102430	Unknown	EX
NPC2g	CG11314	104942	Sterol binding protein	N
Ugt35b	CG6649	108160	UDP glycosyl transferase	N
Ssp7	CG32667	110126	Unknown	N
CG6503	CG6503	110301	Unknown	N
Tip60	CG6121	22233	Histone acetyltransferase	N
enok	CG11290	37527	Histone acetyltransferase	N
wda	CG4448	34847	Histone acetyltransferase	N
lid	CG9088	103830	Histone demethylase	N
pum	CG9755	101399	RNA binding protein/post-translational repressor	N
pros	CG17228	101477	DNA binding transcription activity	N
chm	CG5229	105542	Histone acetyltransferase,	N
stau	CG5753	106645	dsRNA binding protein,	N
Orb2	CG5735	107153	mRNA binding protein	N
CrebA	CG7450	110650	cAMP response element binding protein	N
Homer	CG11324	100271	Protein binding	N
bs	CG3411	100609	Transcription factor	N
scab	CG8095	100949	Integrin alpha chain	N
rut	CG9533	101759	Adenylyl cyclase	N
nord	CG30418	102254	Fibronectin type III	N
kra	CG2922	102609	Translation initiation factor binding protein	E
Chd3	CG9594	102689	ATP-dependent helicase	N
chic	CG9553	102759	Phosphatidylinositol-4,5-bisphosphate binding	N
Pp2B-	CG9842	103144	Serine/threonine phosphatase	N

14D				
Prosap	CG30483	103592 21216	GKAP/Homer scaffold protein	E E
Fas2	CG3665	103807	Neural cell adhesion molecule	N
tws	CG6235	104167	Protein phosphatase type 2A	N
CanB2	CG11217	104370	Serine/threonine phosphatase	N
Nmdar1	CG2902	104773	Ionotropic glutamate receptor	N
HP1c	CG6990	104893	Chromatin binding protein	N
spoon	CG3249	105107	A-kinase anchor protein	N
shn	CG7734	105643	Transcription factor	E
gry	CG17569	105660	unknown	N
fat-spondin	CG6953	105844	Serine-type endopeptidase inhibitor	N
Zasp52	CG30084	106177	Alpha-actinin binding	N
PKD	CG7125	106255	Ca^{2+}/Calmodulin protein kinase	N
mrt	CG3361	106951	Unknown	N
rg	CG44835	107056 36404	Protein kinase A binding protein	N N
PP2A-B'	CG7913	107057	Protein phosphatase A	N
pst	CG8588	107243	Unknown	N
rogdi	CG7725	107310	Unknown	E
Mob2	CG11711	107327	Protein kinase binding protein	N
Ank2	CG42734	107369 40638 46224 107238	Cytoskeletal binding protein	E E N N
cher	CG3937	107451	Actin binding protein	N
sra	CG6072	107573	Protein binding protein	N
CG5846	CG5846	107793	Unknown	E
GluRIA	CG8442	108019	Ionotropic glutamate receptor	N
14-3-3ε	CG31196	108129	Protein kinase C inhibitor	N
ERR	CG7404	108349	Nuclear hormone receptor	N
HDAC6	CG6170	108831	Histone deacetylase	N
crc	CG8669	109014	Transcription factor	N
rl	CG12559	109108	MAP kinase	N
dlg1	CG1725	109274	Guanylate kinase/L-type calcium channel beta subunit	N
Dl	CG3619	109491	Notch binding protein	N
CG42684	CG42684	109589	Ras GTPase-activating protein	N
ben	CG18319	109638	Ubiquitin E2 conjugating enzyme	N
CanA-14F	CG9819	109858	Protein serine/threonine phosphatase	N
Akap200	CG13388	109996	Protein kinase A binding protein	N
tsr	CG4254	110599	Actin-depolymerising factor	EX
Moe	CG10701	110654	Cytoskeletal binding protein	E
Actn	CG4376	100719	Actin and calcium ion binding protein	N
Fmr1	CG6203	110800	RNA binding protein	N
CanB	CG4209	21611	Calcium dependent serine/threonine phosphatase	N
Sir2	CG5216	23201	Histone deacetylase	N
Ank	CG1651	25945	Cytoskeletal protein binding	E
Ranbp21	CG12234	31706	Ran GTPase binding protein	E
mars	CG17064	32841	microtubule binding protein	N
Pp1-87B	CG5650	35025	Serine/threonine phosphatase	N

mts	CG7109	35171	Serine/threonine phosphatase	N
AnxB10	CG9579	36107	Calcium-dependent phosopholipid binding protein	N
Abp1	CG10083	38331	Actin binding protein	N
trio	CG18214	40138	Rho guanyl-nucleotide exchange factor	E
nemy	CG8776	40803	Carbon monoxide oxygenase	N
Kr	CG3340	40871	Transcription factor	N
β-Spec	CG5870	42053	Cytoskeletal protein	N
Appl	CG7727	42673	Amyloidogenic glycoprotein	N
Parp	CG40411	46745	ADP-ribosyltransferase	N
Scamp	CG9195	9130	Unknown	E
Imp	CG1691	20321	mRNA binding protein	E
Lat	CG4088	103716	Origin recognition complex, subunit3	N
StnA	CG12500	105203	Protein binding protein	N
rad	CG44424	101811	RAP-GTPase activating protein	N
Camta	CG42332	106025	Transcription factor	N
hiw	CG32592	26998	E3 ubiquitin ligase	E
amn	CG11937	5606	G-protein coupled receptor binding	E
S6kII	CG17596	101451	Serine/threonine kinase	N
NT1	CG42576	108894	Cystine-knot cytokine	N
Sra-1	CG4931	108876	Rho-GTPase binding protein	E
Bap55	CG6546	24703	Transcriptional co-activator	N
RyR	CG10844	109631	Ryanodine-sensitive calcium release channel	N
stnB	CG12473	24548	Clathrin adaptor	N
NetB	CG10521	100840	EGF-like, laminin	E
G9a	CG2995	110662	histone-lysine N-methyltransferase activity	N
Nf1	CG8318	109637	Ras GTPase activating protein	N
Notch	CG3936	100002	Transmembrane receptor	EX
Adf1	CG15845	102176	Transcription factor	N
nmo	CG7892	104885	Serine/threonine kinase	N
hig	CG2040	13266	Unknown	N
drl	CG17348	27053	Receptor tyrosine kinase	E
cer	CG10460	22752	Cysteine-type endopeptidase inhibitor	E
osk	CG10901	107546	Unknown	N
Ulp1	CG12359	31744	SUMO protease	E
Su(var)2-10	CG8068	30709	DEAD/H-box helicase RNA binding protein; zinc ion binding protein	E
Uba2	CG7528	110173	E1 activating enzyme subunit	E
Aos1	CG12276	47256	E1 activating enzyme subunit	N

The first 16 genes listed have been previously identified to interact with *HDAC4* in other tissues or model systems. Genes on rows 17 to 27 (beginning with *kek2*) were identified in the RNAseq analysis. Abbreviations: REP, rough eye phenotype; E, enhanced; N, no effect, EX, excluded; VDRC ID, Transformant ID number from the Vienna Drosophila Resource Center; Numbers followed by (BDSC) are stock numbers of fly stocks obtained from the Bloomington Drosophila Stock Center; Dom neg, dominant negative construct.